Endoplasmic Reticulum Export Sites and Golgi Bodies Behave as Single Mobile Secretory Units in Plant Cells [W]

Luis L.P. daSilva,[a] Erik L. Snapp,[b] Jürgen Denecke,[a] Jennifer Lippincott-Schwartz,[b] Chris Hawes,[c] and Federica Brandizzi[c,1,2]

[a] Centre of Plant Sciences, University of Leeds, Leeds LS2 9JT, United Kingdom

[b] Cell Biology and Metabolism Branch, National Institute of Child Health and Human Development,
National Institutes of Health, Bethesda, Maryland 20892

[c] Research School of Biological and Molecular Sciences, Oxford Brookes University, Oxford OX3 0BP, United Kingdom

In contrast with animals, plant cells contain multiple mobile Golgi stacks distributed over the entire cytoplasm. However, the distribution and dynamics of protein export sites on the plant endoplasmic reticulum (ER) surface have yet to be characterized. A widely accepted model for ER-to-Golgi transport is based on the sequential action of COPII and COPI coat complexes. The COPII complex assembles by the ordered recruitment of cytosolic components on the ER membrane. Here, we have visualized two early components of the COPII machinery, the small GTPase Sar1p and its GTP exchanging factor Sec12p in live tobacco (*Nicotiana tabacum*) leaf epidermal cells. By in vivo confocal laser scanning microscopy and fluorescence recovery after photobleaching experiments, we show that Sar1p cycles on mobile punctate structures that track with the Golgi bodies in close proximity but contain regions that are physically separated from the Golgi bodies. By contrast, Sec12p is uniformly distributed along the ER network and does not accumulate in these structures, consistent with the fact that Sec12p does not become part of a COPII vesicle. We propose that punctate accumulation of Sar1p represents ER export sites (ERES). The sites may represent a combination of Sar1p-coated ER membranes, nascent COPII membranes, and COPII vectors in transit, which have yet to lose their coats. ERES can be induced by overproducing Golgi membrane proteins but not soluble bulk-flow cargos. Few punctate Sar1p loci were observed that are independent of Golgi bodies, and these may be nascent ERES. The vast majority of ERES form secretory units that move along the surface of the ER together with the Golgi bodies, but movement does not influence the rate of cargo transport between these two organelles. Moreover, we could demonstrate using the drug brefeldin A that formation of ERES is strictly dependent on a functional retrograde transport route from the Golgi apparatus.

INTRODUCTION

In eukaryotic cells, the machinery dedicated to protein secretion is thought to be highly conserved. Secretory proteins enter the secretory pathway in the endoplasmic reticulum (ER), where they undergo folding and assembly reactions. They then traffic to the Golgi apparatus for further processing and sorting to different final destinations (Palade, 1975).

A widely accepted model for ER-to-Golgi transport is based on the sequential action of the COPII and COPI coat complexes. COPII-coated vesicles are responsible for anterograde cargo transport, whereas COPI vesicles have been implicated in both anterograde and retrograde transport (reviewed in Barlowe,

2002). The multisubunit COPII complex is assembled onto the ER membrane in an ordered manner. Before COPII coat assembly, an integral ER membrane protein, Sec12p (Barlowe and Schekman, 1993), acts as a specific guanine nucleotide exchange factor for the activation of Sar1p, a small GTP binding protein (Barlowe and Schekman, 1993; Weissman et al., 2001) and is excluded from the COPII vesicles (Barlowe et al., 1994). The exchange of GDP for GTP on Sar1p triggers the exposure of its N-terminal amphipathic α-helix that constitutes a membrane anchor to the ER (Huang et al., 2001; Bi et al., 2002). The second consequence of the shift in conformation is an increased affinity to the Sec23/24p complex, which leads to the formation of the prebudding complex. The last component to bind to the surface of the nascent coat is the Sec13/31p protein complex (Matsuoka et al., 2001), and COPII vesicle formation is driven by the polymerization of the coat complex, which shapes the bud into a vesicle (Salama et al., 1993, 1997; Barlowe et al., 1994; Matsuoka et al., 1998; Springer and Schekman, 1998). The Sec13/31p acts as a GTPase activating protein and accelerates the GTP hydrolysis on Sar1p by the Sec23/24p (Antonny et al., 2001, 2003). This hydrolysis determines the uncoating of the formed vesicle, and delivery of cargo to the Golgi apparatus occurs through Rab1-dependent tethering and various fusion factors (Allan et al., 2000; Moyer et al., 2001).

The interaction between the cytosolic tails of integral membrane cargo proteins, Sar1p and the Sec23/24p complex, is also thought to mediate cargo selection and concentration into COPII vesicles (Balch et al., 1994; Aridor et al., 1998; Kuehn et al., 1998; Springer and Schekman, 1998). However, specific ER export signals of soluble cargo such as yeast invertase or carboxypeptidaseY are elusive, and it is possible that only a subset of COPII cargo molecules carries active export signals.

COPII-mediated ER export gives rise to the formation of ER export sites (ERES), which are specialized regions of the ER dedicated to sort proteins for export to the Golgi bodies (Aridor et al., 1999, 2001; Hammond and Glick, 2000). In contrast with Sec12p, Sar1p, and the COPII coat components, the features of ERES also vary significantly between different cell types and across kingdoms. In vertebrate cells, ERES appear as specific discrete domains of the ER with a vesicular appearance with the highest density at the perinuclear region, where the ER faces the Golgi ribbon (Palade, 1975; Hong and Tang, 1993). The COPII sorting machinery components are enriched in these areas in distinct vesiculo-tubular structures devoid of ribosomes (Bannykh et al., 1996; Hauri et al., 2000). In the yeast *Pichia pastoris*, Golgi stacks are adjacent to discrete ERES that contain COPII coat proteins and Sec12p (Rossanese et al., 1999).

In plants, the morphology and distribution of ERES is completely unknown, but considerable evidence indicates that components of the COPI and COPII systems operate in protein trafficking in plants (Bar-Peled and Raikhel, 1997; Andreeva et al., 2000; Pimpl et al., 2000; Phillipson et al., 2001; Ritzenthaler et al., 2002). Plant homologs of Sar1p, Rab1p, and Arf1p have been cloned, and *trans*-dominant negative mutants have been used to inhibit protein transport in vivo (Andreeva et al., 2000; Batoko et al., 2000; Takeuchi et al., 2000, 2002; Phillipson et al., 2001; Lee et al., 2002; Pimpl et al., 2003). In addition, the Sar1p-specific exchange factor Sec12p has been characterized and proven to be a useful tool to manipulate COPII-mediated ER export (Phillipson et al., 2001). COPI-coated vesicles, enriched with ER resident HDEL proteins, have been generated in vitro, and their ultrastructure was described in situ via detailed electron microscopy (Movafeghi et al., 1999; Pimpl et al., 2000). However, the unambiguous identification of COPII vesicles and coats analogous to the yeast vesicles and mammalian export site coats remains elusive.

Despite the conservation in secretory machinery, the physical organization of the Golgi apparatus differs enormously across kingdoms. In vertebrate cells, the Golgi apparatus is centrally situated in the perinuclear region of the cell, over the microtubule organizing center. In plant cells, the Golgi apparatus is organized as numerous small cisternal stacks scattered in the cortical cytoplasm and within *trans*-vacuolar strands of cytoplasm (Boevink et al., 1998; Nebenführ et al., 1999). As revealed by fluorescent protein constructs, individual Golgi bodies are closely associated with the cortical ER network (Boevink et al., 1998; Brandizzi et al., 2002; Saint-Jore et al., 2002).

A distinct feature of the plant Golgi apparatus is the mobility of individual cisternal stacks. In leaves, Golgi bodies track along an underlying ER network (Boevink et al., 1998). Moreover, the ER tubules undergo continuous remodeling through the cytoplasm (Boevink et al., 1999). This dynamic organization of the plant

secretory pathway gave rise to two models describing how ER-to-Golgi protein transport may occur in plants. It was proposed that Golgi bodies move between fixed ERES in an actin-myosin–dependent fashion (stop-and-go model; Nebenführ et al., 1999). This model suggests that Golgi bodies become competent for cargo collection once they come to a halt on an ERES upon transient detachment from actin. An alternative model envisages that individual Golgi bodies move to continually collect vesicles budding from the ER (vacuum cleaner model; Boevink et al., 1998). This would suggest that the entire ER surface is export competent. However, both models were not based on measurement of cargo transport, and a recent study of ER-to-Golgi protein transport in vivo has suggested that Golgi body movement is not a prerequisite for ER-to-Golgi protein transport (Brandizzi et al., 2002). To test the two models further, it is essential to identify ERES in plants and to localize these with respect to individual Golgi bodies.

In this study, we have exploited fluorescent-tagged proteins to investigate the distribution and dynamics of ERES in tobacco (*Nicotiana tabacum*) leaf epidermal cells. Using fluorescent protein chimaeras of the GTPase Sar1p and its exchange factor, Sec12p, we have gained insights into the dynamic regulation of secretion, and we have identified putative ERES. We show that Sar1p is recruited onto the sites of protein export when coexpressed with Golgi membrane proteins, and these sites are closely linked, but physically distinct, from the Golgi bodies. Both exchange of Sar1p at the sites of protein export and secretion occur while Golgi stacks move on the ER, but inhibition of COPI-mediated retrograde transport by the drug brefeldin A (BFA) quickly abolishes the formation of Sar1p recruiting ERES. Our findings suggest that the sites of protein export and Golgi membranes behave as a single secretory unit that is motile along the ER.

RESULTS

Sar1-Yellow Fluorescent Protein Exhibit Similar Effects on the Secretory Pathway as Untagged Native Sar1p

To visualize ERES in plant cells, we have fused the yellow fluorescent protein (YFP) to the C terminus of a key component of the COPII machinery, Sar1p. Such fusions are known to preserve the integrity of the Sar1p N terminus that is crucial for its membrane anchoring (Huang et al., 2001; Bi et al., 2002). We expected that the C-terminal fusion with a fluorescent protein would not alter the distribution of Sar1-YFP relative to endogenous Sar1p.

To test the functionality of Sar1-YFP, we determined whether this fusion protein and a GTP-restricted mutant carrying the H74L substitution were detected as intact fusion proteins and exhibited similar effects on protein secretion as the equivalent untagged Sar1p proteins (Figure 1). We transfected tobacco leaf protoplasts with the secretory marker α-amylase (Phillipson et al., 2001) and a dilution series of either Sar1p, Sar1[H74L]p, Sar1-YFP, and Sar1[H74L]-YFP. Figures 1A and 1B show that neither Sar1p nor Sar1-YFP affected α-amylase secretion, similar to previous observations demonstrating that Sar1p
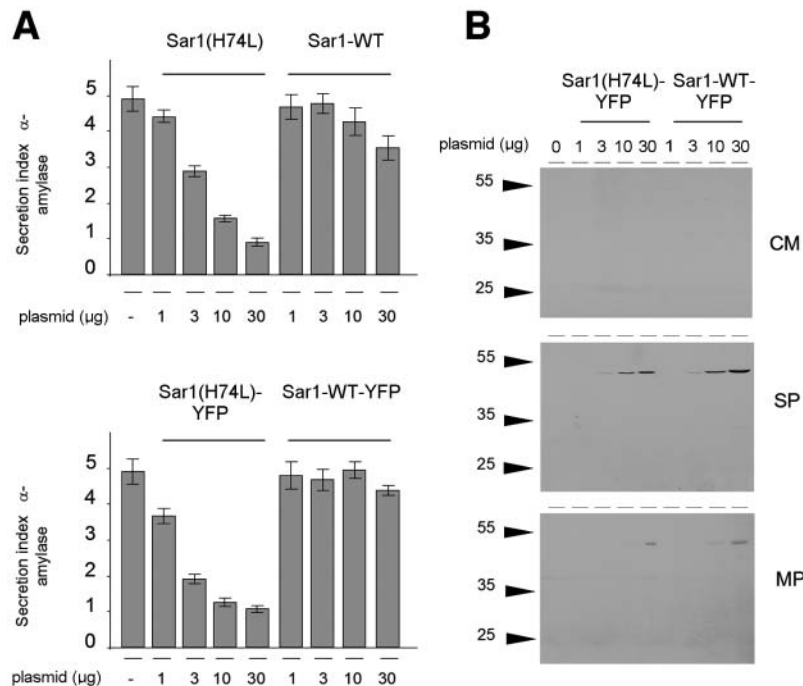
Figure 1. The Fluorescent Sar1p Fusion is Stable and Maintains the Functionality of the Untagged Counterpart.

(A) and **(B)** Transient expression experiment using tobacco leaf protoplasts. Protoplasts were electroporated with a constant amount of plasmid encoding the secretory marker α-amylase and a dilution series of plasmid encoding the effector molecule. **(A)** shows the secretion index of α-amylase (ratio of extracellular and intracellular activities; Phillipson et al., 2001) in protoplasts expressing untagged Sar1[H74L]p and wild-type Sar1p. **(B)** shows a similar experiment, but the untagged GTPase constructs were replaced by the respective C-terminal YFP fusions. Averages of four independent experiments are shown, and error bars are indicated. Note that in **(A)** and **(B)**, coexpression of mutant Sar1p constructs led to a dosage-dependent decline of the secretion index, whereas the wild-type constructs showed hardly any effect, consistent with previous observations (Phillipson et al., 2001).

(C) A representative protein gel blot is shown corresponding to **(B)**, in which the YFP fusions are analyzed. The blots were probed with an anti-GFP serum and demonstrate that Sar1-YFP and its mutant derivative are present as full-length protein fusions, as demonstrated by the size of the bands and the absence of degradation products. Moreover, the fusions were predominantly soluble with greater partition in the soluble phase (SP) of the cell extracts and to a lesser extent in the membrane phase (MP). The absence of protein detected in the concentrated medium (CM) rules out increased cell mortality and leakage of cytosolic YFP fusions to the culture medium.

dosage alone does not affect the secretory pathway (Andreeva et al., 2000; Takeuchi et al., 2000; Phillipson et al., 2001). By contrast, the two molecules with the H74L substitution strongly inhibited the export of the marker (Figures 1A and 1B).

Protein gel blots with an anti–green fluorescent protein (GFP) serum (Figure 1C) indicated that the YFP fusions were present as full-length fusion proteins. The complete absence of degradation products and the similar inhibition profile of tagged and untagged Sar1[H74L]p rules out that proteolytic degradation fragments carrying the native Sar1p moiety were responsible for the effect. Moreover, YFP fusions were predominantly soluble, as shown previously for untagged Sar1p (Phillipson et al., 2001).

Sar1-YFP Is Recruited to Sites Where Golgi Stacks Are Present

To analyze the subcellular distribution of Sar1p, Sar1-YFP was expressed transiently (Figure 2A) or stably (data not shown) in tobacco leaf epidermal cells. In both cases, a diffuse fluorescence was detected in the nucleoplasm (data not shown) and cytoplasm (Figure 2A), surrounding variously shaped and sized organelles, highlighted in negative contrast (Figure 2A, arrows). The distribution of fluorescence in the cytoplasm resembled cytosolic YFP (cYFP; Figure 2B) except for the presence of additional bright punctate structures (Figure 2A, white arrowheads) and ring-like structures (0.5- to 4-μm diameter; Figure 2A, bordered arrowhead).

We hypothesized that a general cytosolic distribution of Sar1-YFP could be linked to a rapid exchange of a small quantity of this protein on the ERES. To test if an increased availability of protein cargo could recruit Sar1p visibly at the ERES, we coexpressed two well-characterized GFP-Golgi markers: the *Arabidopsis thaliana* K/HDEL receptor fusion ERD2-GFP (Boevink et al., 1998; Brandizzi et al., 2002; Saint-Jore et al., 2002) and a GFP fusion with the last 58 amino acids of a rat sialyl transferase, ST-GFP (Boevink et al., 1998; Batoko et al., 2000; Brandizzi et al., 2002; Saint-Jore et al., 2002).
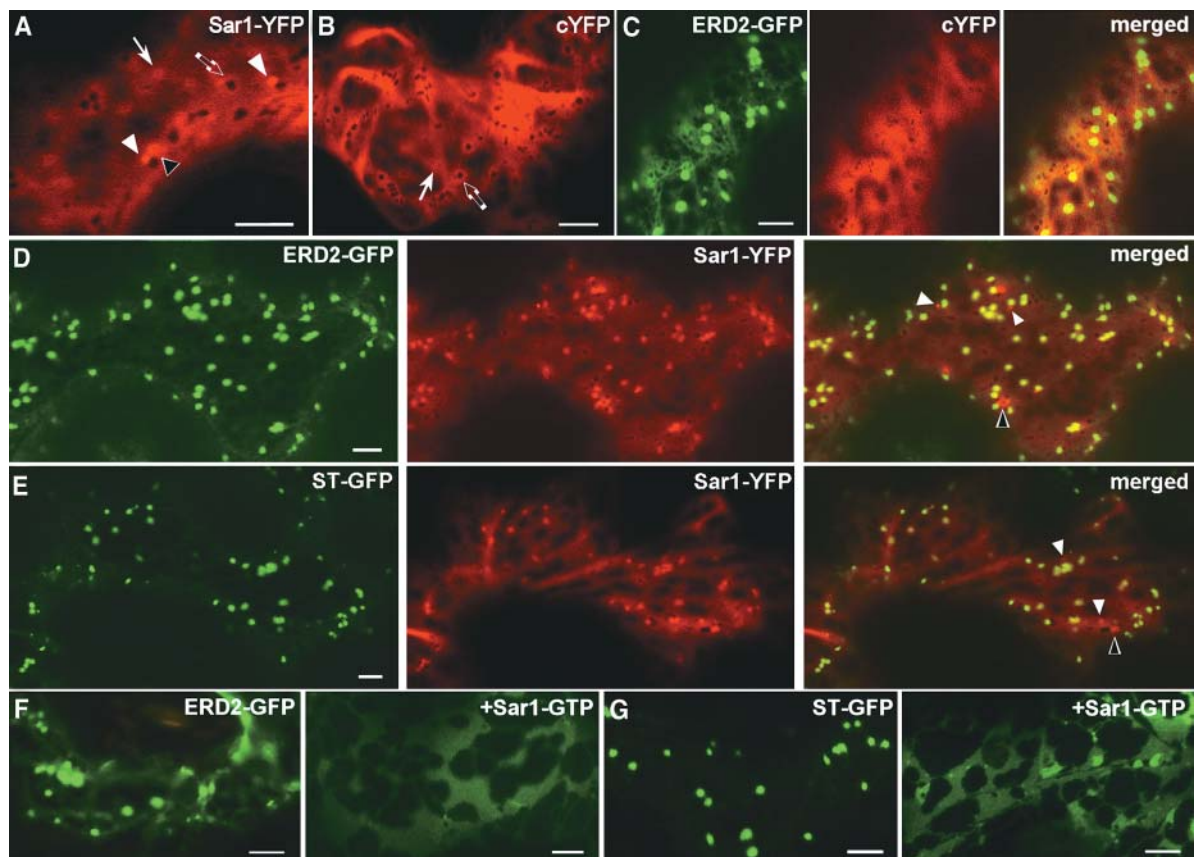
Figure 2. The Subcellular Distribution of a Sar1-YFP Fusion Is Altered by the Expression of Golgi Markers.

(A) and **(B)** Cytoplasm of a tobacco leaf epidermal cell expressing Sar1-YFP (**[A]**; scale bar = 5 μm) and cYFP (**[B]**; scale bar = 2 μm). Open and closed arrows indicate fluorescence accumulations visible in both Sar1-YFP and cYFP that surround organelles, visible in negative contrasts, that are similarly shaped and sized in both cells. White arrowheads point to bright punctate structures, and a bordered arrowhead points at a bright ring-like structure. These structures are observable in Sar1-YFP but not in cYFP-expressing cells.

(C) Epidermal cell coexpressing ERD2-GFP and cytoplasmic YFP (cYFP). Note the absence of accumulation of the YFP fluorescence in punctate structures in the vicinity of individual Golgi bodies. Scale bar = 5 μm.

(D) and **(E)** Coexpression of Sar1-YFP with the Golgi markers ERD2-GFP **(D)** and ST-GFP **(E)**. In cells coexpressing ERD2-GFP and Sar1-YFP **(D)**, the latter maintains a cytosolic pattern but also accumulates in punctate structures in the Golgi body vicinity (scale bar = 5 μm). Comparable to this, in cells coexpressing ST-GFP and Sar1-YFP, the latter is cytosolic but it is also distributed in punctate structures seemingly colocalizing with the Golgi bodies (**[E]**; scale bar = 5 μm). In addition, bright punctate structures (**[D]** and **[E]**, white arrowheads) and ring-like structures (**[D]** and **[E]**, bordered arrowhead) that do not colocalize with a Golgi marker are detectable.

(F) and **(G)** Effect of Sar1[H74L]p on the distribution of Golgi markers. The fluorescence of ERD2-GFP **(F)** and ST-GFP **(G)** is located in the ER upon coexpression of the untagged Sar1p-GTP mutant (scale bar = 5 μm).

These two constructs are known to traffic actively between the ER and the Golgi bodies (Brandizzi et al., 2002; Saint-Jore et al., 2002). We hypothesized that epidermal cells of expanded leaves would have a relatively low secretory activity (in comparison with growing cells), and, therefore, overexpression of these cargo molecules would induce a significant increase in the rate of export out of the ER and increased recycling of the proteins back to the ER. Coexpression of Sar1-YFP with either ERD2-GFP (Figure 2D) or ST-GFP (Figure 2E) resulted in a pronounced punctate appearance of Sar1-YFP in the vicinity of Golgi bodies (Figures 2D and 2E), in addition to the general cytoplasmic staining verified in cells expressing Sar1-YFP alone (Figure 2A). Moreover, additional Sar1-YFP bright punc-

tate and ring-like structures were detected (Figures 2D and 2E, arrowheads). Both these structures did not colocalize nor move synchronously with a GFP-Golgi marker. Similar results were obtained with other known Golgi markers such as a GFP fusion of a sugar transporter, GONST1 (Baldwin et al., 2001; data not shown), and α-1,2 mannosidase I-GFP (Nebenführ et al., 1999; data not shown).

A cYFP construct coexpressed with ERD2-GFP did not reveal punctate structures colocalizing with the Golgi bodies but exhibited a homogeneous cytosolic stain (Figure 2C). This control experiment demonstrates that the punctate subcellular distribution of Sar1-YFP was not a general feature of YFP but was as a result of the Sar1p portion of the fusion protein.
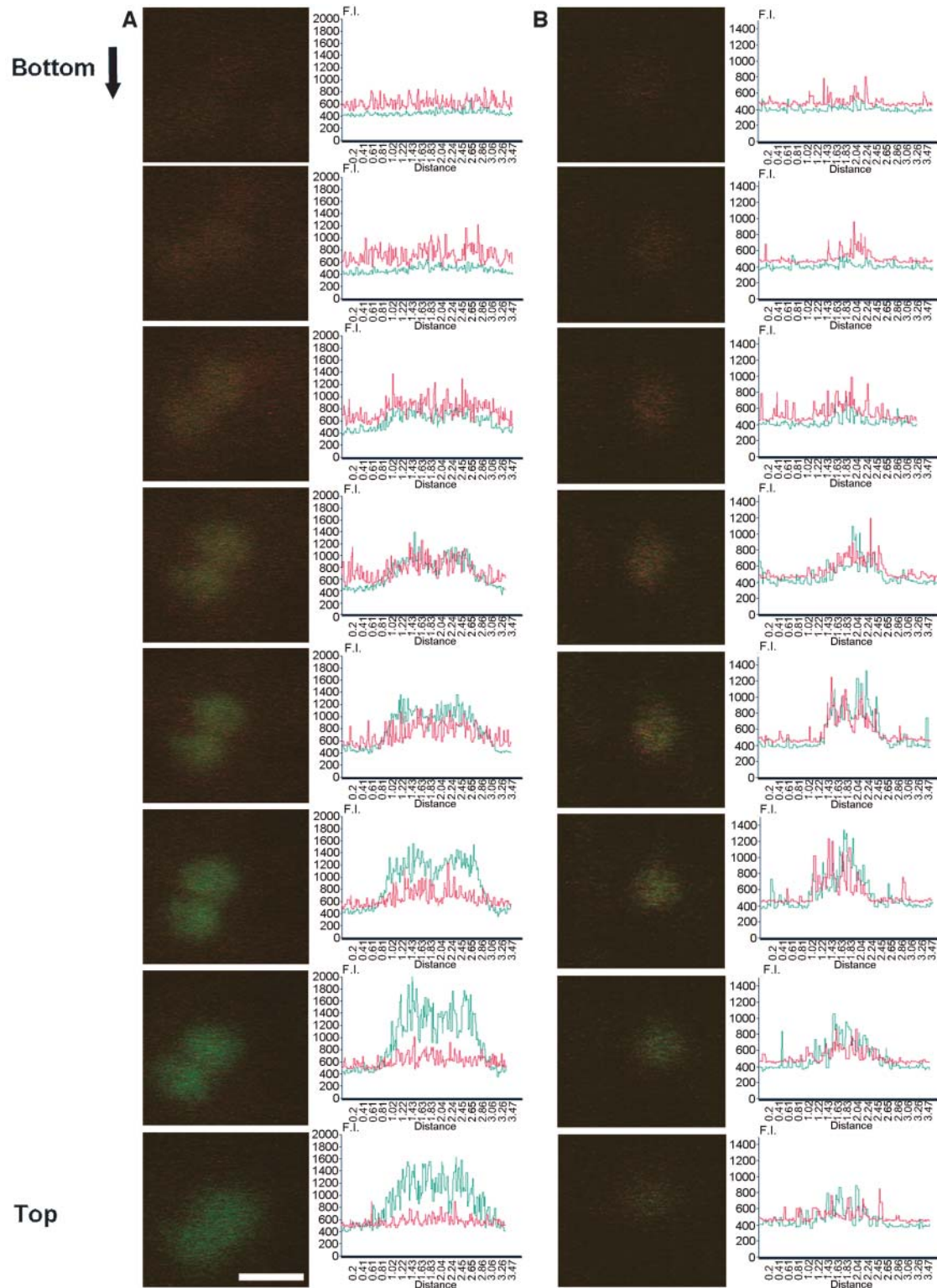
Figure 3. Sar1-YFP Does Not Accumulate All over the Golgi Membranes.

(A) Z-sectioning of a Golgi /Sar1p complex in cells cotransformed with ERD2-GFP and Sar1-YFP and **(B)** of a Golgi complex in cells cotransformed with ERD2-YFP and ERD2-GFP. The fluorescence intensity was measured across the Golgi complex. The graph represents the intensity of fluorescence expressed in arbitrary units (F.I.) along the *y* axis, and the length of the transect along which the fluorescence measurements were gathered is indicated along the *x* axis in microns (Distance). Red line, YFP fluorescence intensity; green line, GFP fluorescence intensity. Bottom indicates the beginning of the z-sectioning, and the following sections move toward the top of the Golgi membranes. Scale bars in **(A)** and **(B)** = 1.5 μm.

We also determined that the export of these Golgi proteins is COPII dependent by coexpressing the dominant negative mutant Sar1[H74L]p, which inhibits α-amylase secretion (Figure 1). Coexpression of this construct with either ERD2-GFP or ST-GFP induces a pronounced ER staining of the Golgi markers (Figures 2F and 2G). Therefore, cycling of both markers includes a COPII-dependent ER export step.

Our combined results indicate that a redistribution of Sar1-YFP from the cytosol to the vicinity of Golgi bodies occurs upon overexpression of Golgi marker proteins, which follow the COPII route to reach the Golgi bodies. This suggests that the cargo may regulate the recruitment of Sar1p at the sites of protein export and initiate COPII-mediated transport.

Sar1-YFP and ERD2-GFP Label Distinct but Overlapping Structures

The close intimacy of Sar1-YFP–labeled structures and Golgi bodies prompted us to analyze the putative ERES/Golgi complex in further detail. We coexpressed Sar1-YFP with the Golgi marker ERD2-GFP, optically sliced the structures highlighted by the two fluorescent markers at the Sar1-YFP/Golgi complex, and collected a series of 0.43-micron optical sections along the z axis of the ERES/Golgi complex, starting from the cytosol toward the Golgi body (Figure 3A). The results show that the signal resulting from Sar1-YFP fluorescence overlaps initially with that of ERD2-GFP but that the ratio between the two fluorophores systematically shifts to ERD2-GFP. Eventually, the signal resulting from Sar1-YFP reduces to the noise value, whereas the ERD2-GFP fluorescence remains high. A control

with an identical optical sectioning procedure on Golgi bodies labeled with ERD2-GFP and ERD2-YFP showed an even distribution of the two fluorochromes across an equivalent region (Figure 3B). The absence of a shift in fluorescence signal observed in this control rules out that the possibility that the Sar1-YFP and ERD2-GFP distributions are the result of chromatic aberrations.

We conclude that Sar1-YFP–labeled loci are physically distinct from the Golgi bodies and represent ERES, and will refer to these as such in the remainder of this article.

The Nature of the Cargo Regulates Sar1-YFP Accumulation at the Golgi Region

Our proposed transport model is attractive because ER export would occur when cargo is present and not as a constitutive measure. However, it was now necessary to ascertain if the accumulation of Sar1-YFP at defined punctate structures could also be triggered by other cargo molecules. In particular, we wanted to test the bulk flow model for ER export, which was shown to occur at least partially via the COPII route (Phillipson et al., 2001). If soluble proteins exit the ER by bulk flow, we predicted that soluble cargo should not recruit Sar1-YFP.

For this purpose, we used an ER-targeted soluble GFP (secGFP; Batoko et al., 2000) that is secreted mostly into the apoplast (Brandizzi et al., 2003). We also coexpressed an ER-targeted and retained soluble GFP, which accumulates in the ER by virtue of the ER retrieval signal HDEL (sGFP-HDEL; Brandizzi et al., 2003). The latter should increase ER export even further because retrieved sGFP-HDEL would continuously
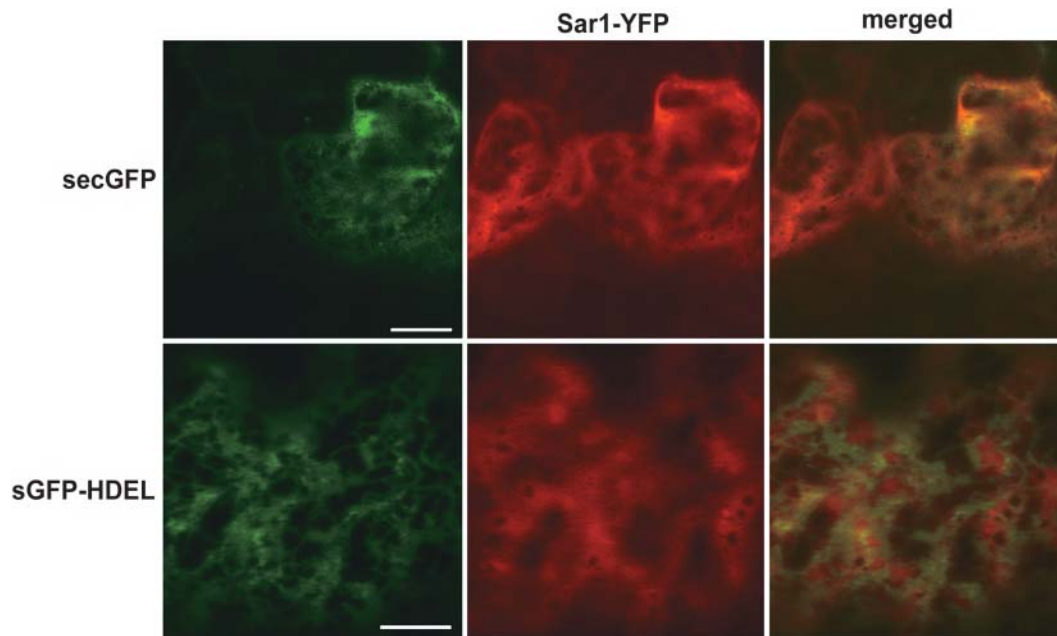

Figure 4. The Subcellular Distribution of Sar1-YFP Is Not Visibly Altered when Soluble Golgi Proteins Are Coexpressed.

Cells coexpressing Sar1-YFP and either secGFP or sGFP-HDEL do not show accumulation of Sar1-YFP in punctate structures similar to those detected upon coexpression of a Golgi marker. Scale bars = 10 μm.

join the de novo synthesized sGFP-HDEL. In contrast with the coexpression experiments with Golgi membrane markers, the cytosolic distribution of Sar1-YFP was not altered in cells coexpressing secGFP or sGFP-HDEL (Figure 4). The lack of accumulation of Sar1-YFP in discrete punctate structures in these cells suggests that soluble cargo, even when present in large quantities by the addition of an HDEL tag, does not visibly recruit the first key element in COPII-dependent transport.

The Sar1p-Guanine Nucleotide Exchange Factor Sec12p Does Not Concentrate at the ERES

To gain further insights on the dynamic regulation of the ER protein export machinery in vivo, we studied the Sar1p-specific guanine nucleotide-exchange factor Sec12p. This protein is an integral ER membrane protein that regulates recruitment of Sar1p onto the ER membranes and the subsequent COPII assembly and is excluded from COPII vesicles (d'Enfert et al., 1991; Barlowe and Schekman, 1993; Barlowe et al., 1994). Therefore, it is an excellent model protein to characterize the ER export process further. To visualize Sec12p in the tobacco leaf system, we fused YFP to the C terminus of Sec12p, to orient the tag in the lumen of the ER, so as not to interfere with the functionality of the cytosolic site of Sec12p.

Overexpression of Sec12p inhibits secretion, likely because of titration of Sar1p (Phillipson et al., 2001). To test whether the Sec12p fusion protein retains the inhibitory effect of its untagged counterpart, we coexpressed untagged Sec12p or Sec12-YFP together with the secretory marker α-amylase in tobacco leaf protoplasts (Figure 5). Figure 5B shows that the fusion protein inhibits α-amylase secretion in a dose-dependent manner, as the untagged Sec12p (Figure 5A). The fusion protein exhibits the expected molecular mass of 70 kD, and it was not possible to detect a degradation product (Figure 5C). This is an essential control as it illustrates that fluorescence microscopy will reveal signals from the fusion protein and not degradation products, which may localize differently. Unlike the Sar1-YFP fusion, most of the Sec12-YFP fusion was detected in the membrane fraction.

Having established this functional aspect of the fusion protein, we now wanted to investigate if Sec12p is enriched at the ERES (Figure 6). When transiently expressed in tobacco leaf epidermal cells, Sec12-YFP localized to the ER (Figure 6A). To probe the mobility of Sec12-YFP in the ER membrane, we photobleached a region of the ER labeled with Sec12-YFP and followed the recovery of the YFP fluorescence in that region (Figure 6A). Upon bleaching, a full recovery of fluorescence within 10 to 20 s from the bleaching event occurred, indicating that Sec12-YFP was highly mobile in the ER membrane (Figure 6A). These data suggested that Sec12-YFP may need to be distributed evenly over the ER membrane to enable rapid exchange of Sar1p at the sites of protein export that are mobile along with the Golgi bodies.

To test this hypothesis, we transiently coexpressed the cargos ERD2-GFP or ST-GFP with low levels of Sec12-YFP that have little or no effect on ER–Golgi transport but can be detected at the ER. This would permit us to analyze, by analogy to Sar1-YFP,
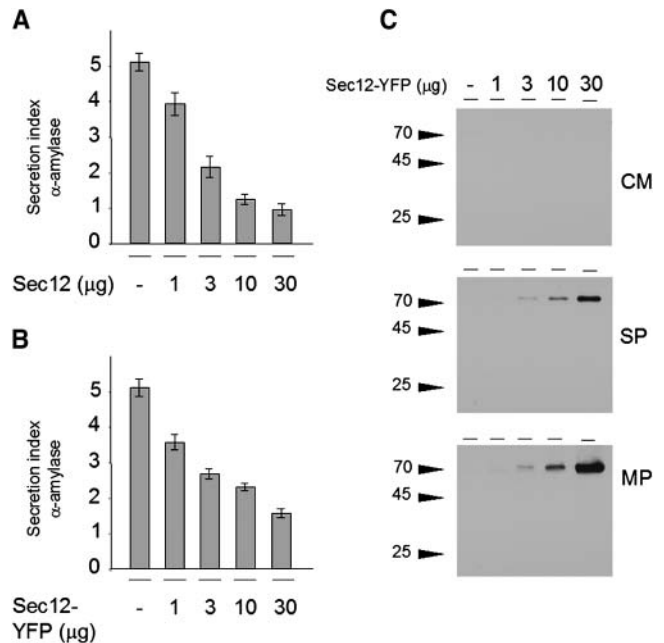

Figure 5. The Fluorescent Fusion of Sec12p, Sec12-YFP, Is Functional as the Untagged Counterpart.

(A) and **(B)** Transient expression experiment using tobacco leaf protoplasts. Protoplasts were electroporated with a constant amount of plasmid encoding the secretory marker α-amylase and a dilution series of plasmid encoding the effector molecule. **(A)** shows the secretion index of α-amylase in protoplasts expressing untagged Sec12p. **(B)** shows a similar experiment but with Sec12p tagged with YFP at its C terminus. Averages of four independent experiments are shown, and error bars are indicated. Note that in both **(A)** and **(B)**, coexpression of the effector led to a dosage-dependent decline of the secretion index.
(C) A representative protein gel blot is shown corresponding to the panel in **(B)** in which the YFP fusion is analyzed. The blots were probed with an anti-GFP serum and demonstrate that Sec12-YFP is present as a full-length protein fusion because it has the correct size and no degradation products were detected. Moreover, in contrast with results with Sar1-YFP fusions (Figure 1C), the Sec12p fusion partitioned predominantly with the membrane phase (MP) rather than in the soluble phase (SP). The absence of protein detected in the concentrated medium (CM) rules out that YFP is proteolytically cleaved in the lumen of the ER and secreted to the medium by bulk flow.

whether specific recruitment of Sec12p to Golgi-associated ERES could be observed in the presence of these cargo proteins. Figures 6B and 6C show that, unlike Sar1p, the exchange factor does not concentrate on the ERES. Under any condition and even at the lowest levels of expression, no localized concentration of Sec12-YFP was detected.

Such an even distribution of Sec12p on the ER network has also been described in *Saccharomyces cerevisiae* (Rossanese et al., 1999) and in mammalian cells (Weissman et al., 2001) but differs from the yeast *P. pastoris*, where discrete ERES contain COPII coat proteins as well as Sec12p (Rossanese et al., 1999).
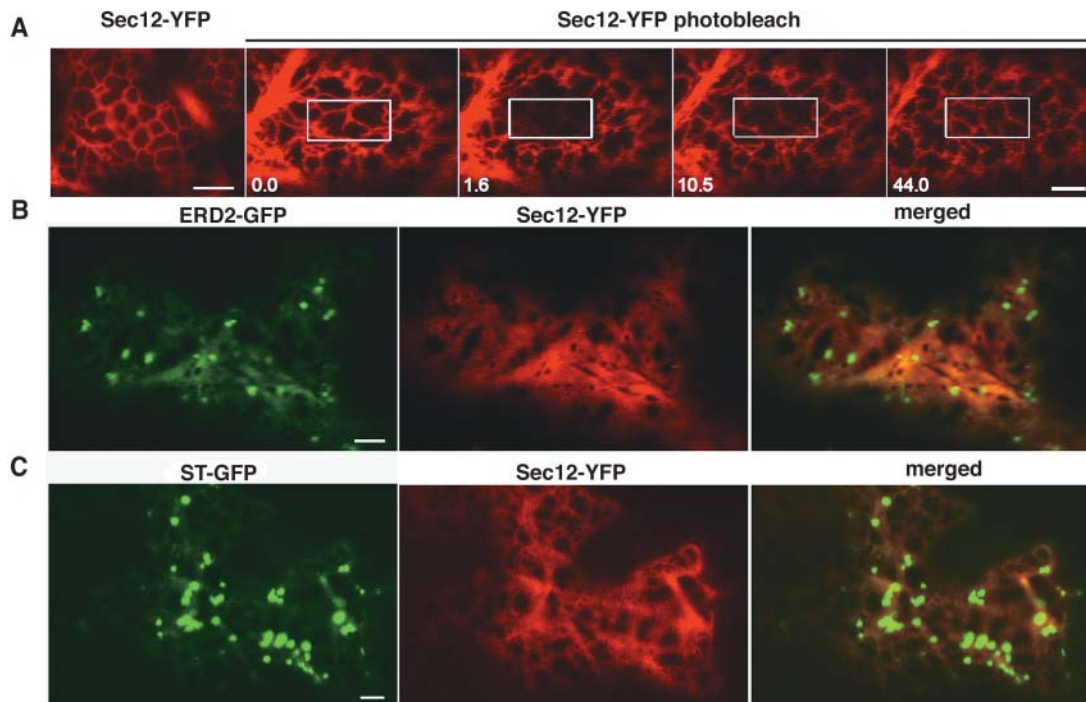
Figure 6. The Sar1p-Specific Guanine Exchange Factor, Sec12p, Distributes in the ER and Moves Freely in the ER Membranes.

(A) Tobacco leaf epidermal cell expressing Sec12-YFP, which labels the ER, and photobleaching of a region of interest (white bordered) of the cortical ER. Time lapse is indicated in seconds at bottom left corner. Note the rapid recovery of fluorescence in the bleached area. Scale bars = 5 μm.
(B) and **(C)** Cell coexpressing Sec12-YFP with either ERD2-GFP **(B)** or ST-GFP **(C)**. Note that Sec12-YFP does not accumulate in discrete punctate structures as Sar1-YFP when coexpressed with a Golgi marker. Scale bars = 5 μm.

Inhibition of ER Export Blocks Sar1-YFP Accumulation on ERES

To investigate whether the accumulation of Sar1-YFP in the vicinity of Golgi bodies is dependent on active secretion and represents a dynamic steady state between recruitment and dissociation of Sar1p via vesicle budding and uncoating, we blocked secretion with either BFA treatment or Sec12p over-expression in leaf epidermal cells coexpressing ERD2-GFP and Sar1-YFP (Figure 7). As expected, BFA treatment results in the rapid absorbance of Golgi membranes and redistribution of GFP-tagged Golgi markers into the ER (cf. Figure 7, −BFA and +BFA; Boevink et al., 1998; Brandizzi et al., 2002; Saint-Jore et al., 2002), an effect that is fully reversible (Saint-Jore et al., 2002). Interestingly, BFA-treated cells also no longer recruited Sar1-YFP to the vicinity of Golgi bodies (Figure 7, +BFA). However, upon washout of BFA, Sar1-YFP accumulated near a reformed Golgi body (Figure 7, BFA recovery). Thus, Sar1-YFP sites are intimately and dynamically associated with the presence of newly formed Golgi bodies and are disrupted by Golgi breakdown induced by BFA. Interestingly, upon BFA treatment, the distribution of Sar1-YFP appeared reticular and closely resembled the distribution of ER labeled with ERD2-GFP in presence of BFA (Figure 7, +BFA).

Overexpression of Sec12p titrates Sar1p and efficiently inhibits COPII-dependent transport (Phillipson et al., 2001). Indeed,

cotransformation of stable transformants expressing either secGFP or ST-GFP with high levels of Sec12-YFP or untagged Sec12p drastically increased accumulation of either protein in the ER (data not shown). This is consistent with the inhibition of α-amylase secretion when large amounts of Sec12p are produced and shows that all three proteins require COPII-mediated transport to leave the ER (Figures 5A and 5B).

We now wanted to test whether inhibition of COPII transport by Sec12p overproduction had an effect on Sar1p accumulation at ERES. We thus coexpressed untagged Sec12p together with ERD2-GFP and Sar1-YFP (Figure 7, +Sec12p). In these conditions, we observed that most of ERD2-GFP was displaced into the ER, and Sar1-YFP fluorescence reduced the appearance in discrete punctate structures. These data are comparable to the results with BFA (Figure 7, +BFA) and indicate that under conditions of disruption of anterograde transport between the ER and the Golgi bodies, Sar1p is no longer recruited to the sites of protein export. Moreover, upon overexpression of untagged Sec12p in cells coexpressing ERD2-GFP and Sar1-YFP, Sar1-YFP fluorescence resembled an ER-like pattern (Figure 7, +Sec12p) in comparison with a control (Figure 7, −BFA). Sec12p distributes at the ER membranes (Figure 6A), and its overexpression titrates Sar1p (Phillipson et al., 2001). Thus, an increased number of Sec12p molecules available for interaction with Sar1-YFP may account for the distribution of the GTPase in a reticulated pattern.
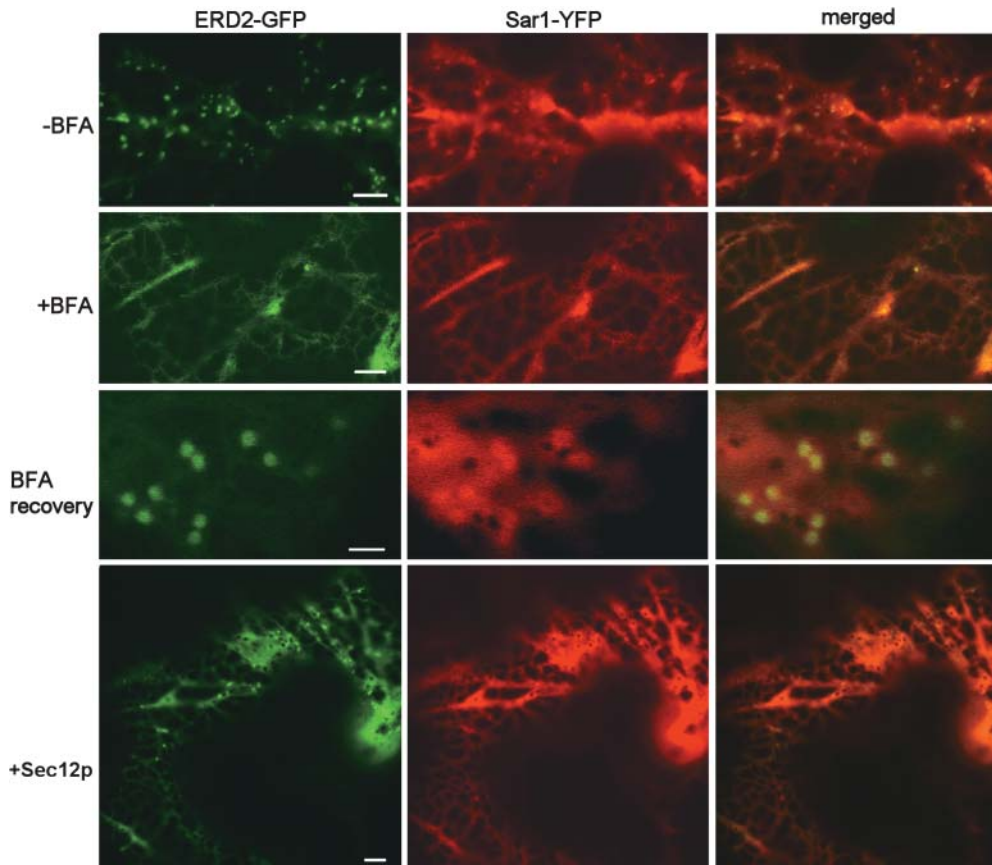
Figure 7. Accumulation of Sar1-YFP at the Golgi Apparatus Vicinity Is Dependent on the Functionality of ER Protein Export.

Cells coexpressing ERD2-GFP and Sar1-YFP show fluorescent Golgi bodies and Sar1-YFP punctate structures (−BFA). Both disappear upon treatment with BFA (100 μg/mL for 1 h; +BFA). This phenomenon is reversible by washing out BFA (BFA recovery). Scale bars = 5 μm. Upon BFA washout, ERD2-GFP redistributes in the Golgi bodies and Sar1-YFP reaccumulates in the vicinity of Golgi bodies. Scale bar = 2 μm. In leaf epidermal cells coexpressing ERD2-GFP, Sar1-YFP and untagged Sec12p (+Sec12p), a reduced accumulation of GFP fluorescence in the Golgi bodies and Sar1-YFP is observed. Scale bar = 5 μm.

Both methods to disrupt protein traffic between the ER and the Golgi apparatus led to the disappearance of the Sar1-YFP–illuminated ERES and provide further evidence for our model.

ERES and Golgi Bodies Move Together as One Secretory Unit

In tobacco leaves and suspension culture tobacco cells, Golgi bodies move on an underlying ER network in an actin-dependent manner (Boevink et al., 1998; Nebenführ et al., 1999; Saint-Jore et al., 2002). When we coexpressed ERD2-GFP and Sar1-YFP, we found that Sar1-YFP bodies moved synchronously within the vicinity of Golgi stacks over the ER (Figure 8).

To determine whether the putative plant ERES highlighted with Sar1-YFP are dependent on similar forces that move the Golgi bodies, we used latrunculin B to depolymerize the actin. Under these conditions, movement of the Sar1-YFP bodies was inhibited along with that of the Golgi stacks, but the two structures remained colocalized (data not shown). This close association of

Golgi stacks with Sar1-YFP accumulation and the absence of Sar1-free Golgi stacks suggest that the Golgi bodies and Sar1-YFP punctate structures behave as a single secretory unit that is mobile along the surface of the ER.

Protein Cargo and Sar1p Exchange during Golgi Bodies Movement

The correlated movement of the Golgi bodies and Sar1-YFP along the surface of the ER suggests that ERES and Golgi stacks form functional units. Combined with the remainder of the data, we hypothesized that increased ER export of membrane cargo is associated with increased Sar1p recruitment from a cytosolic pool to the ERES/Golgi system. To test this hypothesis, we selectively photobleached the YFP and observed its recovery over time, while simultaneously monitoring the movement of the bleached structure using unbleached cyan fluorescent protein (CFP) or GFP fluorescence (Brandizzi et al., 2002). We cotransformed cells with ERD2-CFP and ERD2-YFP and specifically
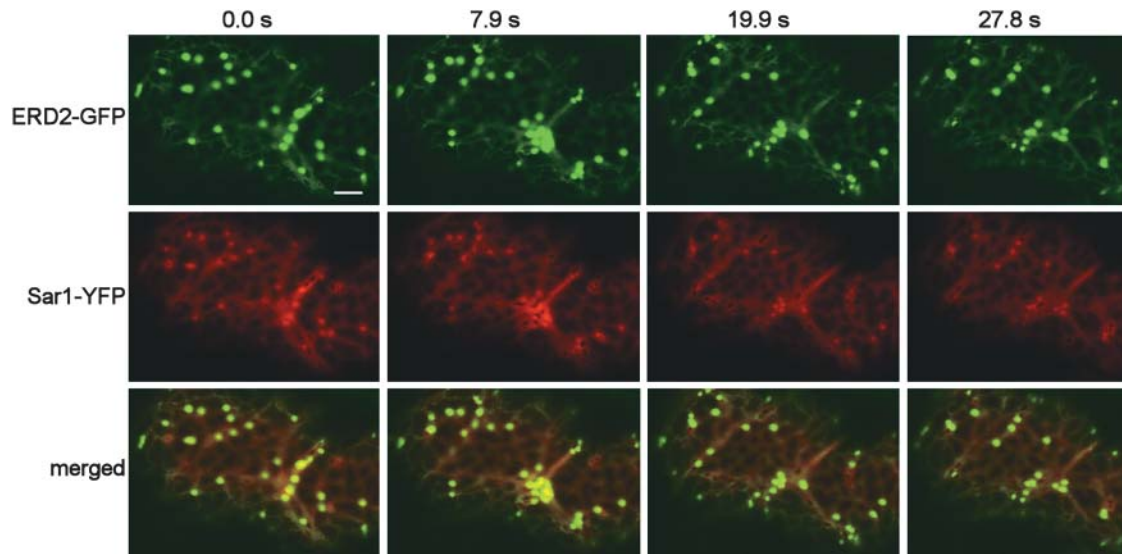
Figure 8. Golgi Stacks and Sar1-YFP Structures Move Together.

Time lapse of a cell cotransformed with ERD2-GFP and Sar1-YFP. Note that Golgi stacks and Sar1-YFP punctate structures move together in the cell at all times. Time of the acquisition of individual frames is indicated on top of ERD2-GFP panels. Scale bar = 5 μm.

bleached YFP fluorescence. Figures 9A and 9C show that YFP fluorescence recovers while Golgi bodies are moving, for example, while the velocity of the Golgi bodies is >0. These data confirm that anterograde cargo can be delivered to moving Golgi bodies.

To test the validity of our hypothesis, we determined whether the COPII machinery is recruited during movement of the ERES. We coexpressed ERD2-GFP with Sar1-YFP and bleached selectively the YFP fluorescence (Figures 9B and 9D). Using the GFP fluorescence as a reference, we could show that the depletion of Sar1-YFP fluorescence within the region of moving Golgi bodies is followed by a rapid recovery (Figures 9B and 9D), indicating that Sar1p can exchange on and off ERES as these structures move in close association with the Golgi bodies along the ER surface.

Sar1p and Golgi Membrane Proteins Exchange at Different Rates

Next, we aimed to compare the dynamics of Sar1p recruitment from the cytosol to ERES with the kinetics of ER-to-Golgi transport of a Golgi membrane marker. Whereas the membrane protein can only reach the Golgi apparatus via membrane-mediated vectors, the GTPase can be recruited directly from the cytosol to the ERES. Thus, we hypothesized that GTPase recruitment would be rapid in comparison with ER–Golgi body transport.

To test this hypothesis, we inhibited Golgi body and ERES movement with latrunculin B, which depolymerizes F-actin as described by Brandizzi et al. (2002), and performed fluorescence recovery after photobleaching (FRAP) experiments on static Golgi bodies and Sar1-YFP structures. This permitted us to

quantify the exchange rate of Sar1-YFP at the ERES in comparison with the exchange rate of the Golgi marker. We used the 458-, 488-, and 514-nm lines of an argon laser to simultaneously photobleach the GFP and the YFP fluorescence, and compared the fluorescence recovery of the two proteins. Upon bleaching, Sar1-YFP fluorescence recovered significantly more rapidly (12.6 ± 6.7 s) than ERD2-GFP fluorescence (105 ± 9.3 s), consistent with an exchange of the Sar1-YFP fluorescence with a cytosolic pool (Figure 10). When simultaneously photobleached, ERD2-YFP and ERD2-GFP fluorescence recovered with equal kinetics (i.e., 105 ± 21.5 s for ERD2-GFP and 106 ± 24.3 s for ERD2-YFP; Figure 10). This result confirmed that the rates of fluorescence recovery are not as a result of the expression of two different fluorochromes.

These data indicate that Sar1p exchanges rapidly from a cytosolic pool and that different cycles of Sar1p membrane binding and release at the ERES are needed for Golgi membrane proteins to exchange an entire Golgi protein pool from the ER.

Impaired GTP Hydrolysis Stabilizes Sar1-YFP Accumulation at the ERES

To further characterize the dynamics of the Sar1p steady state at the plant ERES, we investigated the distribution of the Sar1p-GTP locked mutant (Sar1[H74L]p). The Sar1[H74L]p mutant is still capable of GTP turnover but at a much slower rate than the wild-type counterpart (Aridor et al., 1995).

It is predicted that mutant Sar1-containing COPII vesicles can bud but will accumulate to higher levels before fusion with the Golgi bodies because of a slow shedding of the coat that will retard fusion with the Golgi apparatus. This should result in a more pronounced visualization of a Golgi-associated ERES. To
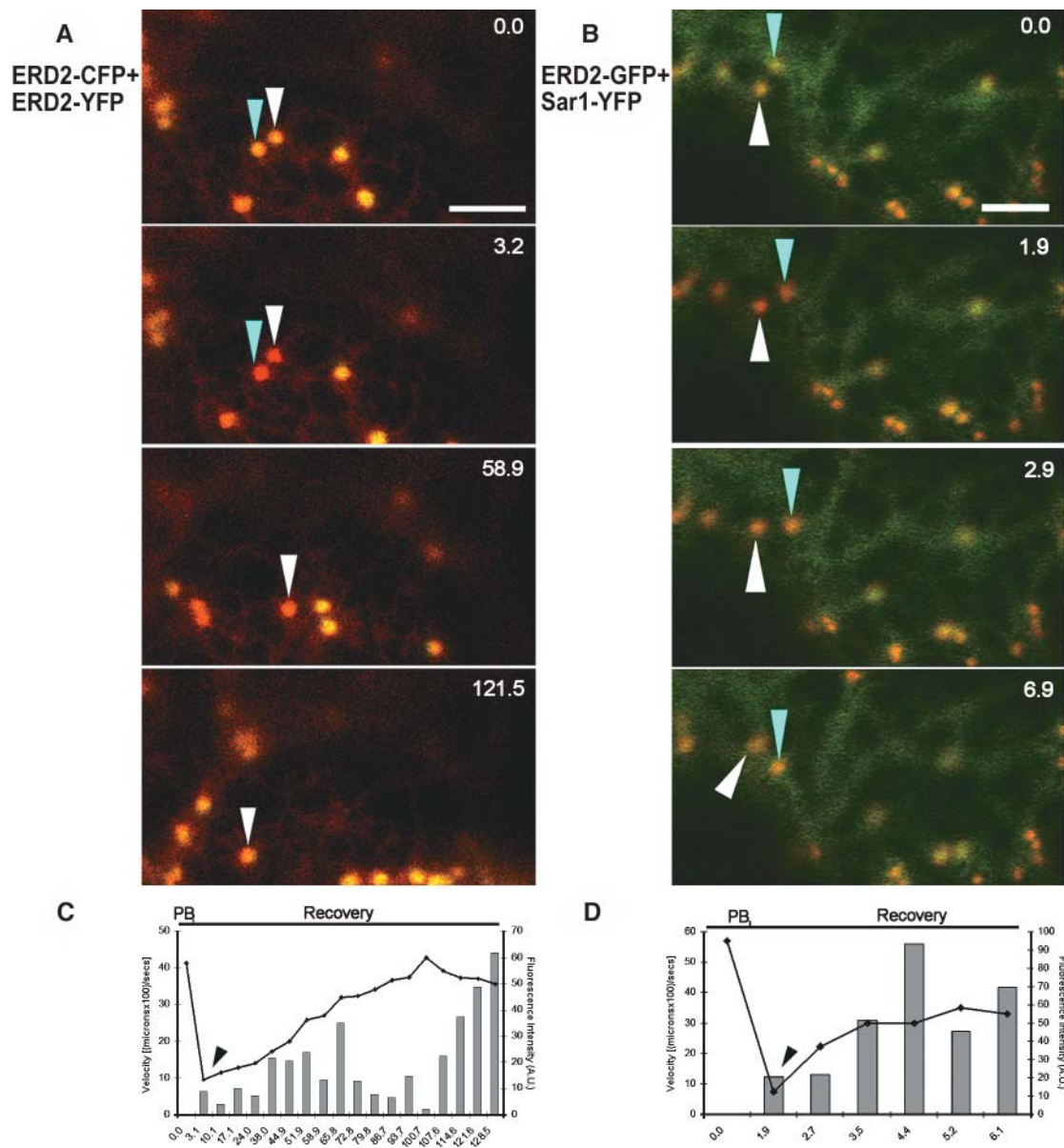
Figure 9. Fluorescent Golgi Markers and Sar1-YFP Exchange Dynamically as the Golgi Bodies Move.

(A) Selective photobleaching of YFP fluorescence of two Golgi bodies (white and blue arrowheads) in a cell cotransformed with ERD2-CFP (pseudocolored in red) and ERD2-YFP (pseudocolored in green). In the merged CFP/YFP prebleaching image (time 0.0 s), the Golgi bodies appear yellow because of the overlapping of the red and green pseudocolors. The first image collected after the YFP bleaching event (3.2 s) shows that both Golgi bodies are now red because of the CFP fluorescence and concomitant loss of the YFP signal. The CFP fluorescence signal remains unaltered after the selective YFP bleaching. Monitoring the red fluorescence resulting from CFP allows continuous tracking of the YFP bleached Golgi bodies and measuring the YFP fluorescence recovery after bleaching. Two images of the postbleaching recovery are reported here to show the fluorescence recovery into the white-arrowed Golgi bodies (58.9 s and 121.5 s). Note that one of the bleached Golgi bodies (blue arrow) moved outside the plane of observation during the course of the experiment.

(B) Selective photobleaching of the fluorescence of two Sar1-YFP structures (arrowheads) in cells cotransformed with Sar1-YFP (pseudocolored in green) and ERD2-GFP (pseudocolored in red). As for the selective photobleaching of YFP in the CFP/YFP combination, the bleaching of YFP in the YFP/GFP couple allows tracking of a YFP bleached structure by monitoring of the GFP signal that remains unaltered upon the bleaching event, and simultaneous computation of the YFP signal. In this sequence, two Sar1-YFP structures (white and blue arrows) have been selected on Golgi bodies labeled with ERD2-GFP for YFP selective bleaching (prebleach, 0.0 s). In the first postbleach image (1.9 s), the Golgi bodies appear mostly pseudocolored in red because of the GFP. A YFP cytosolic background still partially masks the Golgi body fluorescence. In just a few seconds, the YFP fluorescence resulting from Sar1-YFP recovers on the mobile Golgi bodies (see postbleach images at 2.9 and 6.9 s). Note the rapid recovery of Sar1-YFP fluorescence at the Golgi bodies compared with ERD2-YFP recovery in ERD2-YFP and ERD2-CFP bleaching sequence. Time series are indicated in seconds at the right-hand corner. Scale bars = 5 μm.
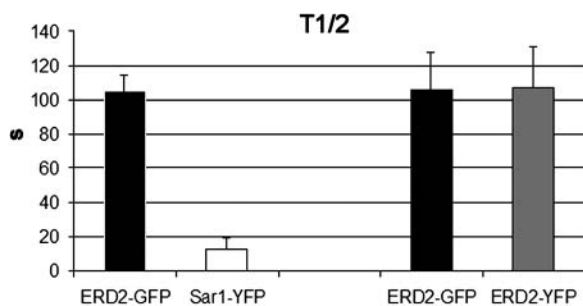
Figure 10. Golgi Membrane Proteins and Sar1-YFP Exchange with Different Kinetics.

Half-time (T1/2) data gathered from FRAP experiments on static Golgi bodies and Sar1-YFP structures to quantify the exchange of Sar1-YFP at the ERES, and to compare it with the dynamics of a Golgi marker. Histograms indicate the half-time of fluorescence recovery after simultaneous photobleaching of ERD2-GFP and Sar1-YFP structures ($n = 10$) and ERD2GFP plus ERD2-YFP ($n = 11$). Data significant for $P = 0.05$. n, Number of repetitions.

test this hypothesis, we expressed a YFP chimaera of the Sar1[H74L]p mutant in tobacco leaf epidermal cells (Sar1-GTP-YFP; Figure 11A) at low levels, to maintain reasonable ER-to-Golgi transport. In these conditions, cells expressing Sar1-GTP-YFP alone displayed numerous discrete mobile punctate structures in comparison with Sar1-YFP alone (Figure 2A). This supports the prediction that Sar1-GTP-YFP, once trapped on the sites of protein export by a slower GTP turnover, accumulates and therefore becomes more visible, even in the absence of the cargo that induces ERES. The results also indicate that Sar1-YFP–labeled ERES represent not only Sar1p-coated ER membranes and nascent COPII structures but also a localized pool of COPII vectors in transit.

To establish whether these Sar1-GTP-YFP structures localized in the vicinity of Golgi bodies and therefore mark the ERES, we expressed low levels of Sar1-GTP-YFP with ERD2-GFP. Under these conditions we observed that Sar1-GTP-YFP colocalized 98% with ERD2-GFP (Figure 11B) and moved with the Golgi bodies (data not shown). This finding supports the hypothesis that ERES and Golgi bodies are associated in plants.

In cells expressing Sar1-GTP-YFP alone at higher levels, the fluorescence of the fusion was mainly restricted to the cytosol with a drastic reduction of the number of punctate structures visible in low-expressing cells (data not shown), suggesting that COPII-mediated protein transport was compromised under these conditions. To confirm that ER export was disrupted under these conditions, we transiently expressed Sar1-GTP-YFP with ERD2-GFP (Figure 11C) or secGFP (Figure 11D), to detect any

alteration in the GFP fluorescence distribution pattern. As with the untagged Sar1p-GTP mutant (Figure 2F; data not shown), overexpression of the Sar1-GTP-YFP caused disappearance of the Golgi bodies in cells coexpressing ERD2-GFP (Figure 11C) and accumulation of fluorescence in the ER in cells coexpressing secGFP (Figure 11D).

These experiments demonstrate that vesicle budding still occurs at a modest concentration of the dominant-negative GTPase. However, at high concentrations of the mutant GTPase, ERES themselves are compromised, possibly by a loss of other essential components, which normally recycle from the Golgi apparatus back to the ER but are now titrated out in fusion-incompetent COPII vectors.

DISCUSSION

In the study of ER-to-Golgi protein transport in plant cells, the mechanisms by which proteins leave the ER for the Golgi apparatus are currently a subject of intense investigation. Evidence has been obtained that soluble proteins can leave the ER by bulk flow (Denecke et al., 1990) and that this includes ER residents that return via their K/HDEL motifs (Phillipson et al., 2001). Currently, no ER export signal has been identified for a plant protein, and although examples of such signals are known in some mammal and yeast proteins, there is also evidence that bulk flow occurs in these systems, and concentration of anterograde cargo in the Golgi apparatus is achieved through selective retrieval of ER components via COPI transport (Klumperman, 2000). In addition, the role of the movement of Golgi bodies in plant cells has remained the source of much speculation (Boevink et al., 1998; Nebenführ et al., 1999).

To describe the process of ER export in more detail, we have followed the dynamics of two regulatory proteins of the COPII machinery and described the behavior of plant ERES in vivo. We found that whereas Sec12p gene product was homogeneously distributed over the ER, regardless of the expression levels, the GTPase Sar1p specifically localized to putative ERES upon coexpression of Golgi membrane markers. This permitted us to analyze whether cargo molecules can influence the frequency and appearance of these sites and how they move in relation to the Golgi bodies.

Cargo Molecules with Exposed Cytosolic Domains Can Trigger the Formation of ERES

Our results show that membrane proteins, which maintain high steady state levels at the Golgi bodies but also cycle between the ER and the Golgi stacks, recruit increased levels of Sar1p to defined punctate structures on the ER network. Because these

---

Figure 9. (continued).

(C) and **(D)** Intensity of fluorescence at the moment of prebleaching (PB), immediately after bleaching (arrowheads), and in the recovery phase in the above experiments for the Golgi bodies indicated with a white arrowhead in **(A)** and a Sar1-YFP structure indicated by a blue arrowhead in **(B)**. Time lapse is expressed in seconds along the *x* axis. Gray histograms show the relative distance covered between two sequential images divided by the time involved in the acquisition of the two images (velocity), and the curve represents the fluorescence intensity of the measured structures normalized to the background fluorescence.
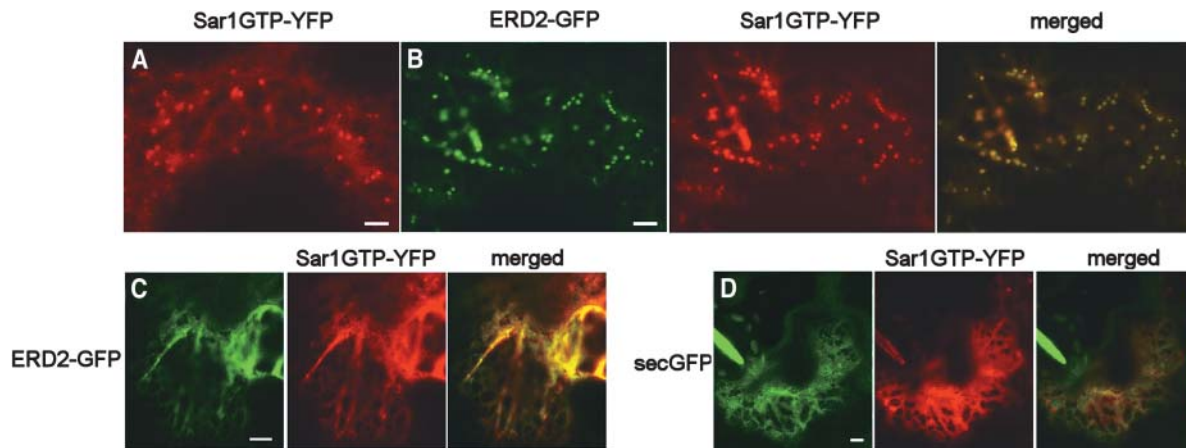
Figure 11. Sar1-GTP-YFP Accumulates in Punctate Structures and Exerts a Dominant Negative Effect on Protein Secretion.

(A) A tobacco leaf epidermal cell expressing low levels of Sar1-GTP-YFP alone (bacterial OD at 600 nm = 0.01) shows punctate structures and cytosolic stain.

(B) Cell coexpressing ERD2GFP and Sar1-GTP-YFP. It is possible to verify that Golgi bodies colocalize with the punctate structures highlighted with Sar1-GTP-YFP (merged).

(C) and **(D)** Cells coexpressing Sar1-GTP-YFP, at higher levels (bacterial OD at 600 nm = 0.05) than cells in **(A)** and **(B)**, and either ERD2-GFP **(C)** or secGFP **(D)**, show GFP accumulation in the ER and a reduced appearance of Sar1-GTP-YFP structures. Note that the confocal microscope settings (laser power and detection gain) for imaging YFP fluorescence in **(C)** and **(D)** are lowered than in **(A)** and **(B)** to reduce oversaturation. Scale bars = 5 μm.

structures were adjacent to the Golgi bodies, we concluded that they represent ERES and that a Sar1-YFP fusion is an excellent tool to visualize these regions. Interestingly, soluble cargo molecules expressed at similar or even higher levels did not induce visible Sar1p recruitment to the ERES. The results indicate that ERES formation and recruitment of Sar1p may depend on the nature of the cargo molecule and not simply its quantity.

Sar1p regulates the recruitment of COPII coat complexes (Sec23/Sec24p and Sec13/Sec31p) onto the ER membranes and promotes vesicle formation from the ER in yeast and mammals (Nakano and Muramatsu, 1989; Oka et al., 1991; Barlowe et al., 1994; Kuge et al., 1994; Oka and Nakano, 1994). However, it has also been suggested that Sar1p may be involved in the selection and concentration of integral membrane proteins at the ERES because of the recognition of specific signals present on the cytosolic tails of specific cargo proteins (Aridor et al., 1998; Springer and Schekman, 1998; Otte and Barlowe, 2002; Giraudo and Maccioni; 2003). Alternatively, cargo proteins may have an active role in modulating COPII coat assembly and vesicle budding in vertebrate cells and in vitro because evidence has been presented showing that the availability of biosynthetic cargo in the ER can either prevent or enhance the formation of COPII vesicles (Aridor et al., 1999).

Our results reveal that overexpression of resident Golgi membrane proteins with regions exposed in the cytosolic domains causes Sar1-YFP accumulation in punctate structures that localize in the vicinity of individual Golgi bodies. This suggests that membrane cargo can stimulate Sar1p accumulation at ERES. This could occur because of an increase in number of cytosolic domains that are recognized by Sar1p. Results obtained with soluble fluorescent protein markers

further support this hypothesis because these markers do not contain regions exposed to the cytosol and the COPII machinery. Upon coexpression of Sar1-YFP with either secGFP or sGFP-HDEL, no Sar1-YFP punctate structures were detected. ER export of sGFP-HDEL should be significant because de novo synthesized protein would be further enriched by recycling proteins; nevertheless, no significant recruitment of Sar1-YFP to ERES could be detected. This is most likely because of the fact that soluble cargo may simply be secreted by bulk flow as shown for secreted or vacuolar hydrolases, or ER resident proteins such as calreticulin (Phillipson et al., 2001). It could be argued that overexpression of an HDEL molecule should recruit more K/HDEL receptor to the ERES and therefore induce formation of Sar1p punctate structures. However, recycling of HDEL proteins is a saturable process, as demonstrated by secretion to post-Golgi compartments of overexpressed calreticulin-HDEL or α-amylase-HDEL, even in stable transformants (Crofts et al., 1999; Phillipson et al., 2001) and sGFP-HDEL (Brandizzi et al., 2003). Therefore, lack of appearance of punctate structures in conditions of overexpression of sGFP-HDEL may be because of a limited pool of available endogenous receptor that would not recruit enough Sar1-YFP at the ERES to make the Sar1p punctate structures detectable.

Interestingly, the Sar1-specific guanine nucleotide exchange factor Sec12p was never concentrated at the ERES, even in the presence of overexpressed Golgi resident membrane proteins, which recruit Sar1p. The result indicates that ERES formation does not depend on a localized concentration of Sec12p. A relatively even distribution of the exchange factor and a high mobility within the ER membranes may be required to permit movement of ERES and associated Golgi bodies.

S. cerevisiae has a dispersed Golgi apparatus and structural COPII proteins are present throughout the cytoplasm, and Sec12p is distributed throughout the ER, suggesting that COPII vesicles may bud from the entire ER network (Nishikawa and Nakano 1991, 1993; Rossanese et al., 1999). This is different from vertebrate ERES, which are dynamic structures that exhibit slow, short-range movements (Hammond and Glick, 2000), whereas the juxtaposed vesicular-tubular clusters have directed long-range movement dependent on microtubules (Presley et al., 1997; Scales et al., 1997), and from the yeast *P. pastoris*, in which Golgi stacks are immobile, coherent, and adjacent to discrete ERES that contain COPII coat proteins as well as Sec12p. It is tempting to speculate that in plants the distribution of Sec12p may reflect a need of the plant secretory system to have a Sar1p exchange factor, Sec12p, distributed all over the ER. This would operate when Golgi bodies and ERES move along the surface of the ER.

Together, our results suggest that the GTPase Sar1p is a suitable marker to highlight the ERES in conditions of coexpression of Golgi bodies membrane proteins, as it may be actively recruited as a consequence of the increased levels of membrane cargo, which contains exposed cytosolic domains. It will be worthwhile to test this in other cell types, particularly those exhibiting high secretory activity.

ERES and Golgi Bodies Are Intimately Associated and Highly Mobile

To determine the nature of the distribution of Sar1-YFP in the vicinity of Golgi bodies, we optically sectioned the Sar1-YFP/ERD2-GFP complex. We have been able to identify a region of Sar1-YFP overlapping with ERD2-GFP and another section above this, which is labeled exclusively with ERD2-GFP. These data indicate that Sar1p is not distributed over the whole Golgi stack and that, in our experimental conditions, ERD2-GFP, which cycles between the ER and the Golgi bodies, is concentrated at higher levels in the Golgi bodies than in ERES at steady state. The interface comprising Sar1-YFP/ERD2-GFP is likely to be a result of a distribution of ERD2-GFP in forming COPII membranes that are decorated with Sar1-YFP on the coat. The HDEL receptor is known to have a high steady state level in the Golgi membranes, but it must be exported from the ER to recycle effectively. Therefore, it is not surprising that the labeling of Sar1-YFP may mimic the area of the Golgi membrane facing the ER. Because of the inherent resolution limits of confocal microscopy, the results obtained do not exclude the possibility that Sar1-YFP binds to the *cis*-face of the individual Golgi bodies. The physical separation of the Golgi bodies from the ER in plant cells is still a matter of debate, and recent literature does not exclude that the Golgi membranes and ER may be connected (Brandizzi et al., 2002). However, there is no published report from any eukaryotic model system that suggests that Sar1p may have a direct affinity to Golgi membranes. Our optical slicing rules out that Sar1-YFP is distributed evenly over the Golgi stack, and our data support all the existing COPII literature indicating that Sar1p binds to the ER and not the Golgi membranes to initiate COPII-mediated transport. Therefore, we concluded that punctate structures illuminated by Sar1-YFP represent ERES.

A detailed investigation of the dynamics of ERES revealed two important observations. ERES and Golgi bodies remain associated during movement on the ER network and, in addition, the Golgi bodies can receive cargo during movement. The latter was shown by applying FRAP to one fluorescent protein in a double-labeled system and demonstrated that Golgi bodies can collect cargo during their movement. Therefore, they do not necessarily have to come to a halt to collect cargo. This is further supported by the demonstration that Sar1-YFP can be rapidly recruited from the cytosol to mobile ERES adjacent to the Golgi bodies during their synchronous movement. These data indicate that Sar1p can exchange on and off ERES as these structures move in close association with the Golgi bodies along the ER surface.

The combined results argue against the stop-and-go model (Nebenführ et al., 1999) that postulated that Golgi stacks stop transiently at ERES to acquire cargo, whereas movement between ERES would be accompanied by a lack of cargo transport. Taken together with previous results showing that Golgi body movement is not a prerequisite for ER-to-Golgi transport (Brandizzi et al., 2002), we can conclude that ERES and Golgi body movement are unrelated to the rate of ER export.

We propose a new model in which both ERES and Golgi bodies form functional units that remain intimately associated. It is an extension of the cisternal maturation model for the Golgi stacks, which holds that ER export gives rise to the formation of *cis*-Golgi cisternae, which mature into medial and *trans*-cisternae by selective retrieval of components through COPI-dependent retrograde transport. Our model extends this view by stating that, in leaf epidermal cells, the ERES and probably the site at which retrograde transport is received by the ER are closely linked and remain associated with individual Golgi stacks. In addition, considering data available in literature, we reason that recovery of Golgi fluorescence in FRAP experiments is not as a result of transport from other Golgi bodies. Tubular connections between two or more Golgi bodies have not been seen in leaves, and there is no record of Golgi-to-Golgi vesicle carriers. Also, any retrograde COPI vesicle carriers percolating through the stack are most likely tethered and in the in vivo situation would not be free to fuse with adjacent stacks (Barr and Short, 2003). Even if vesicle transport occurs between two Golgi bodies, it would not be so efficient to give rise to the recovery rates observed here and by Brandizzi et al. (2002), simply because of the considerable distance between different Golgi stacks, which also varies enormously between different Golgi bodies.

In cells expressing Sar1-YFP alone, it is possible to identify punctate and ring-like structures. When we coexpressed Sar1-YFP with either ERD2-GFP or ST-GFP, we verified that all the Golgi stacks associated with a Sar1-YFP punctate structure. In addition, other Sar1-YFP punctate and ring-like structures did not colocalize visibly with a Golgi marker. One possible explanation is that these structures may represent the sites where new Golgi bodies form. In this model, a Golgi body would always associate with an ERES; however, we cannot exclude that additional ERES are present in a cell. The presence of forming ERES that lack Golgi membranes strongly supports the idea that

Sar1-YFP does not label the Golgi bodies but rather an ER domain.

Regulation of Transport Is Determined by COPII and COPI Integrity

Our model also predicts that Golgi stacks are simply a consequence of ER export and not preexisting structures that seek and find ERES. The necessary protein traffic associated with retrieving retrograde cargo from anterograde cargo is a much more likely explanation for its existence. Consistent with this, inhibition of ER export, either through the indirect effect of the drug BFA (Boevink et al., 1998; Robineau et al., 2000; Brandizzi et al., 2002; Ritzenthaler et al., 2002; Saint-Jore et al., 2002) or the direct inhibition of COPII vesicle budding by overproduction of either Sec12p or Sar1p-GTP restricted mutant (Andreeva et al., 2000; Takeuchi et al., 2000; Phillipson et al., 2001), abolished accumulation of Sar1-YFP at the ERES and simultaneously caused Golgi bodies to become undetectable. Photobleaching experiments of Golgi bodies in BFA-treated cells have indicated that BFA may interfere directly with ER–Golgi protein transport before reabsorption of Golgi membranes into the ER occurs (Brandizzi et al., 2002). Here, BFA treatment of cells coexpressing Sar1-YFP and Golgi membrane markers caused Sar1-YFP punctate structures to disperse and Golgi membrane proteins to redistribute into the ER. This effect was reversible, as BFA washout was followed by reformation of the Golgi bodies and the Sar1-YFP structures.

Combined with our previous photobleaching data on BFA-treated cells (Brandizzi et al., 2002), the new data suggest that BFA treatment prevents ERD2-GFP or ST-GFP from recruiting Sar1-YFP to the ERES. Thus, the sequential activity of the Sar1-COPII and of Arf1p-coatomer systems jointly serve to form and maintain forward protein transport to the Golgi bodies, whose components continuously circulate through the ER. Although it is not clear which factors become limiting during BFA treatment, it has been shown that BFA releases Arf1p from Golgi membranes (Pimpl et al., 2000), and it is reasonable to assume that the activity of Arf1p-coatomer is required for forward trafficking out of the ER because of its role in recycling essential components needed for the COPII-dependent ER export. Interestingly, upon BFA treatment, the distribution of Sar1-YFP resembled an ER-like pattern. It is possible that factors other than Sar1p are required for ERES formation, and BFA-induced defective COPI recycling followed by fusion of Golgi apparatus and ER membranes may cause the dispersal of Sar1p along the ER–Golgi supercompartment.

To gain further insight into the regulation of protein export from the ER, we coexpressed a GTP-restricted mutant of Sar1p (Sar1[H74L]p) as a fusion with YFP (Sar1-GTP-YFP). It is well documented that such a mutant blocks secretion in BY-2 cells, Arabidopsis suspension culture cells, or tobacco protoplasts and plants (Andreeva et al., 2000; Takeuchi et al., 2000; Phillipson et al., 2001). Similar observations were made with soluble cargo transported to the lytic vacuole (Takeuchi et al., 2000), which accumulated in the ER when the mutant was coexpressed. Overexpression or microinjection of Sar1p-GTP in vertebrate cells has the same effect (Kuge et al., 1994; Shima

et al., 1998; Zaal et al., 1999; Ward et al., 2001). Our current experiments confirm this effect in plant cells.

Interestingly, cells coexpressing low levels of Sar1-GTP-YFP and a Golgi marker show colocalization of the two constructs, proving that the mutant also marks ER domains adjacent to the Golgi bodies. In fact, the fluorescence of Sar1-GTP-YFP accumulates at the ERES at low levels, even without the triggering effect of cargo molecules. It has been suggested that as a result of the ability of GTP-restricted Sar1p to inhibit COPII uncoating, COPII coated vesicles fail to develop into mature vesicular-tubular clusters and appear attached to each other as beads on a string confined to ERES (Bannykh et al., 1996). The mutant Sar1p was also shown to efficiently reconstitute ER vesicle formation in the presence of COPII components Sec23/24p and Sec13/31p and leads to the accumulation of COPII-coated vesicles in vivo and in vitro (Aridor et al., 1995, 1998; Rowe et al., 1996). At the resolution of confocal microscopy, we cannot establish the ultrastructural nature of the accumulated Sar1-GTP-YFP. However, it can be concluded that ERES are still highlighted by the mutant Sar1p fusion. Nonetheless, at high concentrations of the GTP-restricted mutant Sar1p, no export sites were seen and Golgi markers were fully retained in the ER, thus that continuous production of COPII vectors trapped in their coated configuration leads to loss of ER export altogether. This result suggests that an essential factor must be titrated from the ER membrane, which prevents further ERES formation and causes Sar1-GTP-YFP to remain cytosolic.

Conclusion

The work presented in this article addresses the complex issue of ERES/Golgi dynamics in plant cells. The visualization of putative ERES has been achieved by live cell imaging using fluorescent chimaeras of the COPII coat initiator Sar1p in conditions of coexpression of Golgi membrane proteins. We define an ERES as a region in which Sar1p-coated ER membrane forms concentrated loci, which contain nascent COPII membranes as well as COPII vectors in transit. In addition, the existence of Sar1-YFP punctate structures separated from Golgi bodies does not exclude the existence of isolated ERES. This article illustrates the dynamic nature of plant ERES and shows their intimate association with the Golgi bodies. The occurrence of ER-to-Golgi transport during the joint movement of the ERES–Golgi system requires the postulation of a new model, which is an extension of the cisternal maturation model of the Golgi apparatus. The biological function of the actin-mediated movement of this system remains to be established but does not seem to be related to the transport of cargo molecules between the ER and the Golgi bodies. Interestingly, the work also presents evidence for active recruitment of Sar1p to ERES by cargo molecules, but this only applies to membrane proteins with exposed cytosolic domains. Soluble cargo molecules did not cause increased recruitment of the COPII machinery to ERES, which provides strong arguments in favor of the bulk flow model for soluble proteins in plants.

Future studies in our laboratory will concentrate on the molecular and ultrastructural characterization of the ERES in different cell types.

METHODS

Molecular Cloning and *Agrobacterium tumefaciens* Transformation

Standard molecular techniques were used as described by Sambrook et al. (1989). The fluorescent proteins used in this study were based on fusions with either mGFP5 (Haseloff et al., 1997), ECFP, or EYFP (Clontech, Palo Alto, CA). The spectral properties of mGFP5 allow efficient spectral separation from YFP (Brandizzi et al., 2002).

For *Agrobacterium tumefaciens* transient expression of untagged tobacco (*Nicotiana tabacum*) Sar1p and its GTP mutant (Andreeva et al., 2000), we used the binary vector pVKH18-En6 (Batoko et al., 2000), and we inserted the DNA coding sequence of the two proteins within the unique *Xba*I and *Sac*I sites of the vector. For *A. tumefaciens* transient expression of Sec12p, the 35S-Sec12-3′nos chimeric gene (Phillipson et al., 2001) was inserted as an *Eco*RI (partial *Hind*III) fragment directly into the polylinker of the binary plant vector pDE1001 (Denecke et al., 1992) cut with *Eco*RI and *Hind*III, followed by dephosphorylation. The resulting vector permits *A. tumefaciens*–mediated plant transformation using kanamycin resistance but also works in a 2- to 3-d infiltration essay without selection.

For *A. tumefaciens* transient expression of fluorescent constructs, the coding sequence of tobacco Sar1p and its GTP mutant (Andreeva et al., 2000) and Arabidopsis Sec12p (Phillipson et al., 2001) were inserted upstream YFP, using the unique *Xba*I and *Sal*I sites of the vector. To generate sGFP-HDEL, the coding region of a sporamin signal peptide fused in frame with GFP5 and HDEL (Brandizzi et al., 2003) was inserted in pVKH18En6 between the unique *Xba*I and *Sac*I sites of the binary vector.

The primer sequences used for the subcloning indicated above are available upon request.

Plant Material and Transient Expression Systems

Four-week-old tobacco (cv Petit Havana) greenhouse plants grown at 25°C were used for *A. tumefaciens* (strain GV3101)–mediated transient expression (Batoko et al., 2000). The bacterial OD used for plant transformation was 0.01 to 0.05 for tagged and untagged versions of Sar1p, Sar1p-GTP mutant, and Sec12p, and 0.2 for ST- and ERD2-tagged constructs, secGFP, and sGFP-HDEL.

For transient expression in protoplasts, tobacco plants (cv Petite Havana) were grown in MS medium (Sigma, St. Louis, MO) and 2% sucrose in a controlled room at 25°C with a 16-h-light/8-h-dark regime at the light irradiance of 200 mE m^{-2} s^{-1}. Tobacco leaf protoplast preparation and subsequent DNA transfection via electroporation were performed as described by Phillipson et al. (2001), and the plasmid concentrations used are given in the figures. After electroporation, the protoplasts were incubated for 24 h.

After the appropriate incubation time, the suspension was spun for 5 min at 100*g* in a swing-out centrifuge (4K15; Sigma), which results in the floating of the cells. Using an extrafine Pasteur pipette, we removed 1 mL of clear supernatant from below the floating cell layer. The remainder of the suspension (1 mL) was brought to 10 mL with 250 mM NaCl and mixed gently by inverting the tube twice. After a second spin of 5 min at 100*g*, the supernatant was removed with a peristaltic pump, and the cell pellet was placed on ice. The cells were extracted in a final volume of 250 μL. Equal volumes of cell extract and culture medium were analyzed by protein gel blotting or by enzymatic analysis.

Protein Gel Blot Analysis

Protein analysis of culture medium was performed after concentration with aqueous ammonium sulfate solution (60% final) on ice, using BSA at 0.5 mg/mL as a carrier. The protein precipitate was then resuspended in α-amylase extraction buffer, concentrating the culture medium samples 10-fold compared with the original volume. Cell proteins were analyzed separately as soluble phase and pelleted membranes. The analysis of soluble cell proteins was conducted after sonication of the protoplasts in α-amylase extraction buffer and centrifugation for 10 min at 25,000*g* at 4°C. The supernatant containing the soluble proteins was recovered. The pellet containing membrane proteins was resuspended by brief sonication. Both cell protein samples were resuspended to a 10-fold lower volume than the original cell suspension in α-amylase extraction buffer.

Protein cell extracts or concentrated medium were loaded in equal volumes after 2× dilution with 2× SDS loading buffer (Crofts et al., 1999) and boiling. Protein in SDS–polyacrylamide gels were transferred onto a nitrocellulose membrane and then blocked with PBS, 0.5% Tween 20, and 5% milk powder for 1 h. The filter was then incubated in blocking buffer with primary antibody at a dilution of 1:10,000 for the anti-GFP serum and 1:5000 for the anti-IgG antibody. All the antisera were from rabbits, and further steps were performed as by Crofts et al. (1999).

α-Amylase Assay

The cells were extracted in α-amylase extraction buffer (Crofts et al., 1999) via sonication for 5 s. The extracts were centrifuged 10 min at 25,000*g* at 4°C, and the clean soluble supernatant was recovered. The culture medium was also spun 10 min at 25,000*g* at 4°C to remove residual cell debris. The α-amylase assays and calculation of the secretion index were performed as described previously (Crofts et al., 1999; Phillipson et al., 2001). The secretion index represents the ratio between the extracellular and intracellular activity, and the total activity corresponds to the sum of the activity detected in the medium and in the cells (Denecke et al., 1990).

Drug Treatments

Segments (roughly 5 mm^2) of transformed leaves were used for drug treatment, confocal imaging, and analysis. For actin depolymerization, leaf tissue was submerged in 25 μM latrunculin B (stock solution: 10 mM in DMSO; Calbiochem, Nottingham, UK) for 1 h. BFA (stock solution: 10 mg/mL in DMSO; Sigma-Aldrich, London, UK) was used at a concentration of 100 μg/mL as described by Brandizzi et al. (2002). BFA washes were performed as described earlier (Brandizzi et al., 2002). All stock solutions were kept at −20°C, and working solutions were prepared fresh just before use.

Sampling and Imaging

Transformed leaves were analyzed 48 h after infection of the lower epidermis. Confocal imaging was performed using an inverted Zeiss 510 laser scanning microscope and an upright Zeiss 510 META (Jena, Germany) and a 63× oil and water immersion objective. For imaging expression of either GFP constructs or YFP constructs or both, we used imaging setting as described by Brandizzi et al. (2002) with a 3-μm pinhole diameter. Similarly, coimaging of CFP and YFP construct expression was done according to Brandizzi et al. (2002). In both cases, appropriate controls were done to exclude the possibility of energy transfer between fluorochromes and cross talk. In control experiments, we also used ERD2-YFP and ST-YFP in combination with Sar1-GFP and obtained accumulation of Sar1-GFP structures in the vicinity of Golgi bodies as for Sar1-YFP detected in coexpression of GFP–Golgi markers. Time-lapse scanning was acquired with imaging system software of the microscope.

For optical sectioning the ERES/Golgi bodies complex, the optimal diameter pinhole was determined according to the manufacturer's instructions to produce the best signal/noise ratio, and was set to 1 Airy unit (<0.9 μm for GFP and <1.0 μm for YFP). Increments on the *z* axis of

the ERES/Golgi complex were set at 0.43 μm. Fluorescence intensity measurements (plus tracking) and postacquisition image processing were done with Zeiss confocal and PaintShop Pro 7.0 software (Jasc Software, Eden Prairie, MN), respectively.

Photobleaching Recovery Studies

Spot photobleaching recovery measurements were performed on an inverted Zeiss LSM 510 confocal microscope. FRAP experiments for dual fluorochrome photobleaching and half-time computation were performed as by Brandizzi et al. (2002). Significance statistics was determined using a Student's two-tailed t test for two samples assuming equal variance.

As for the selective photobleaching of YFP in the CFP/YFP and GFP/YFP combinations, the method for selective YFP fluorescence bleaching was adapted from Brandizzi et al. (2002). For this, we used the 514-nm laser line of an argon laser while imaging either the CFP or GFP fluorescence with the argon 458-nm laser line in cells in which the Golgi body movement was not altered by the use of any drug. A small region of interest (4 to 9 μm²) containing one or two target structures was selected in a cell coexpressing YFP and either GFP or CFP, and the fluorescence of YFP was bleached using a brief pulse of 100% 514-nm laser line. The YFP and GFP/CFP intensity of the fluorescence of the organelles of interest was recorded before the bleaching event and in the time after the bleaching event until fluorescence recovery plateau was achieved. This bleaching protocol leaves the fluorescence resulting from either GFP or CFP unaltered. Bleaching of YFP in the YFP/CFP or YFP/GFP couple allows monitoring of the CFP/GFP signal and simultaneous tracking and computation of the YFP signal recovery on a CFP/GFP-labeled structure with the fast scanning multitracking facility of the confocal microscope.

REFERENCES

Allan, B.B., Moyer, B.D., and Balch, W.E. (2000). Rab1 recruitment of p115 into a cis-SNARE complex: Programming budding COPII vesicles for fusion. Science **289,** 444–448.

Andreeva, A.V., Zheng, H., Saint-Jore, C.M., Kutuzov, M.A., Evans, D.E., and Hawes, C.R. (2000). Organization of transport from endoplasmic reticulum to Golgi in higher plants. Biochem. Soc. Trans. **28,** 505–512.

Antonny, B., Gounon, P., Schekman, R., and Orci, L. (2003). Self-assembly of minimal COPII cages. EMBO Rep. **4,** 419–424.

Antonny, B., Madden, D., Hamamoto, S., Orci, L., and Schekman, R. (2001). Dynamics of the COPII coat with GTP and stable analogues. Nat. Cell Biol. **3,** 531–537.

Aridor, M., Bannykh, S.I., Rowe, T., and Balch, W.E. (1995). Sequential coupling between COPII and COPI vesicle coats in endoplasmic reticulum to Golgi transport. J. Cell Biol. **131,** 875–893.

Aridor, M., Bannykh, S.I., Rowe, T., and Balch, W.E. (1999). Cargo can modulate COPII vesicle formation from the endoplasmic reticulum. J. Biol. Chem. **274,** 4389–4399.

Aridor, M., Fish, K.N., Bannykh, S., Weissman, J., Roberts, T.H., Lippincott-Schwartz, J., and Balch, W.E. (2001). The Sar1 GTPase coordinates biosynthetic cargo selection with endoplasmic reticulum export site assembly. J. Cell Biol. **152,** 213–229.

Aridor, M., Weissman, J., Bannykh, S., Nuoffer, C., and Balch, W.E. (1998). Cargo selection by the COPII budding machinery during export from the ER. J. Cell Biol. **141,** 61–70.

Balch, W.E., McCaffery, J.M., Plutner, H., and Farquhar, M.G. (1994). Vesicular stomatitis virus glycoprotein is sorted and concentrated during export from the endoplasmic reticulum. Cell **76,** 841–852.

Baldwin, T.C., Handford, M.G., Yuseff, M.I., Orellana, A., and Dupree, P. (2001). Identification and characterization of GONST1, a Golgi-localized GDP-mannose transporter in *Arabidopsis*. Plant Cell **13,** 2283–2295.

Bannykh, S.I., Rowe, T., and Balch, W.E. (1996). The organization of endoplasmic reticulum export complexes. J. Cell Biol. **135,** 19–35.

Bar-Peled, M., and Raikhel, N.V. (1997). Characterization of AtSEC12 and AtSAR1. Proteins likely involved in endoplasmic reticulum and Golgi transport. Plant Physiol. **114,** 315–324.

Barlowe, C. (2002). COPII-dependent transport from the endoplasmic reticulum. Curr. Opin. Cell Biol. **14,** 417–422.

Barlowe, C., and Schekman, R. (1993). SEC12 encodes a guanine-nucleotide-exchange factor essential for transport vesicle budding from the ER. Nature **365,** 347–349.

Barlowe, C., Orci, L., Yeung, T., Hosobuchi, M., Hamamoto, S., Salama, N., Rexach, M.F., Ravazzola, M., Amherdt, M., and Schekman, R. (1994). COPII: A membrane coat formed by Sec proteins that drive vesicle budding from the endoplasmic reticulum. Cell **77,** 895–907.

Barr, F.A., and Short, B. (2003). Golgins in the structure and dynamics of the Golgi apparatus. Curr. Opin. Cell Biol. **15,** 405–413.

Batoko, H., Zheng, H.Q., Hawes, C., and Moore, I. (2000). A Rab1 GTPase is required for transport between the endoplasmic reticulum and Golgi apparatus and for normal Golgi movement in plants. Plant Cell **12,** 2201–2218.

Bi, X., Corpina, R.A., and Goldberg, J. (2002). Structure of the Sec23/24-Sar1 pre-budding complex of the COPII vesicle coat. Nature **419,** 271–277.

Boevink, P., Martin, B., Oparka, K., Cruz, S.S., and Hawes, C. (1999). Transport of virally expressed green fluorescent protein through the secretory pathway in tobacco leaves is inhibited by cold shock and brefeldin A. Planta **208,** 392–400.

Boevink, P., Oparka, K., Santa Cruz, S., Martin, B., Betteridge, A., and Hawes, C. (1998). Stacks on tracks: The plant Golgi apparatus traffics on an actin/ER network. Plant J. **15,** 441–447.

Brandizzi, F., Hanton, S., DaSilva, L.L., Boevink, P., Evans, D., Oparka, K., Denecke, J., and Hawes, C. (2003). ER quality control can lead to retrograde transport from the ER lumen to the cytosol and the nucleoplasm in plants. Plant J. **34,** 269–281.

Brandizzi, F., Snapp, E.L., Roberts, A.G., Lippincott-Schwartz, J., and Hawes, C. (2002). Membrane protein transport between the endoplasmic reticulum and the Golgi in tobacco leaves is energy dependent but cytoskeleton independent: Evidence from selective photobleaching. Plant Cell **14,** 1293–1309.

Crofts, A.J., Leborgne-Castel, N., Hillmer, S., Robinson, D.G., Phillipson, B., Carlsson, L.E., Ashford, D.A., and Denecke, J.

(1999). Saturation of the endoplasmic reticulum retention machinery reveals anterograde bulk flow. Plant Cell **11,** 2233–2248.

d'Enfert, C., Barlowe, C., Nishikawa, S., Nakano, A., and Schekman, R. (1991). Structural and functional dissection of a membrane glyco-protein required for vesicle budding from the endoplasmic reticulum. Mol. Cell. Biol. **11,** 5727–5734.

Denecke, J., Botterman, J., and Deblaere, R. (1990). Protein secretion in plant cells can occur via a default pathway. Plant Cell **2,** 51–59.

Denecke, J., De Rycke, R., and Botterman, J. (1992). Plant and mammalian sorting signals for protein retention in the endo-plasmic reticulum contain a conserved epitope. EMBO J. **11,** 2345–2355.

Giraudo, C.G., and Maccioni, H.J. (2003). Endoplasmic reticulum export of glycosyltransferases depends on interaction of a cytoplas-mic dibasic motif with Sar1. Mol. Biol. Cell **14,** 3753–3766.

Hammond, A.T., and Glick, B.S. (2000). Dynamics of transitional endoplasmic reticulum sites in vertebrate cells. Mol. Biol. Cell **11,** 3013–3030.

Haseloff, J., Siemering, K.R., Prasher, D.C., and Hodge, S. (1997). Removal of a cryptic intron and subcellular localization of green fluorescent protein are required to mark transgenic *Arabidopsis* plants brightly. Proc. Natl. Acad. Sci. USA **94,** 2122–2127.

Hauri, H.P., Kappeler, F., Andersson, H., and Appenzeller, C. (2000). ERGIC-53 and traffic in the secretory pathway. J. Cell Sci. **113,** 587–596.

Hong, W., and Tang, B.L. (1993). Protein trafficking along the exocytotic pathway. Bioessays **15,** 231–238.

Huang, M., Weissman, J.T., Beraud-Dufour, S., Luan, P., Wang, C., Chen, W., Aridor, M., Wilson, I.A., and Balch, W.E. (2001). Crystal structure of Sar1-GDP at 1.7 A resolution and the role of the NH2 terminus in ER export. J. Cell Biol. **155,** 937–948.

Klumperman, J. (2000). Transport between ER and Golgi. Curr. Opin. Cell Biol. **12,** 445–449.

Kuehn, M.J., Herrmann, J.M., and Schekman, R. (1998). COPII-cargo interactions direct protein sorting into ER-derived transport vesicles. Nature **391,** 187–190.

Kuge, O., Dascher, C., Orci, L., Rowe, T., Amherdt, M., Plutner, H., Ravazzola, M., Tanigawa, G., Rothman, J.E., and Balch, W.E. (1994). Sar1 promotes vesicle budding from the endoplasmic reticulum but not Golgi compartments. J. Cell Biol. **125,** 51–65.

Lee, M.H., Min, M.K., Lee, Y.J., Jin, J.B., Shin, D.H., Kim, D.H., Lee, K.H., and Hwang, I. (2002). ADP-ribosylation factor 1 of *Arabidopsis* plays a critical role in intracellular trafficking and maintenance of endoplasmic reticulum morphology in *Arabidopsis*. Plant Physiol. **129,** 1507–1520.

Matsuoka, K., Orci, L., Amherdt, M., Bednarek, S.Y., Hamamoto, S., Schekman, R., and Yeung, T. (1998). COPII-coated vesicle formation reconstituted with purified coat proteins and chemically defined liposomes. Cell **93,** 263–275.

Matsuoka, K., Schekman, R., Orci, L., and Heuser, J.E. (2001). Surface structure of the COPII-coated vesicle. Proc. Natl. Acad. Sci. USA **98,** 13705–13709.

Movafeghi, A., Happel, N., Pimpl, P., Tai, G.H., and Robinson, D.G. (1999). *Arabidopsis* Sec21p and Sec23p homologs. Probable coat proteins of plant COP-coated vesicles. Plant Physiol. **119,** 1437–1446.

Moyer, B.D., Allan, B.B., and Balch, W.E. (2001). Rab1 interaction with a GM130 effector complex regulates COPII vesicle cis-Golgi tethering. Traffic **2,** 268–276.

Nakano, A., and Muramatsu, M. (1989). A novel GTP-binding protein, Sar1p, is involved in transport from the endoplasmic reticulum to the Golgi apparatus. J. Cell Biol. **109,** 2677–2691.

Nebenführ, A., Gallagher, L.A., Dunahay, T.G., Frohlick, J.A.,

Mazurkiewicz, A.M., Meehl, J.B., and Staehelin, L.A. (1999). Stop-and-go movements of plant Golgi stacks are mediated by the acto-myosin system. Plant Physiol. **121,** 1127–1142.

Nishikawa, S., and Nakano, A. (1991). The GTP-binding Sar1 protein is localized to the early compartment of the yeast secretory pathway. Biochim. Biophys. Acta **1093,** 135–143.

Nishikawa, S., and Nakano, A. (1993). Identification of a gene required for membrane protein retention in the early secretory pathway. Proc. Natl. Acad. Sci. USA **90,** 8179–8183.

Oka, T., and Nakano, A. (1994). Inhibition of GTP hydrolysis by Sar1p causes accumulation of vesicles that are a functional intermediate of the ER-to-Golgi transport in yeast. J. Cell Biol. **124,** 425–434.

Oka, T., Nishikawa, S., and Nakano, A. (1991). Reconstitution of GTP-binding Sar1 protein function in ER to Golgi transport. J. Cell Biol. **114,** 671–679.

Otte, S., and Barlowe, C. (2002). The Erv41p-Erv46p complex: Multiple export signals are required in trans for COPII-dependent transport from the ER. EMBO J. **21,** 6095–6104.

Palade, G. (1975). Intracellular aspects of the process of protein synthesis. Science **189,** 347–358.

Phillipson, B.A., Pimpl, P., daSilva, L.L., Crofts, A.J., Taylor, J.P., Movafeghi, A., Robinson, D.G., and Denecke, J. (2001). Secretory bulk flow of soluble proteins is efficient and COPII dependent. Plant Cell **13,** 2005–2020.

Pimpl, P., Hanton, S.L., Taylor, J.P., Pinto-daSilva, L.L., and Denecke, J. (2003). The GTPase ARF1p controls the sequence-specific vacuolar sorting route to the lytic vacuole. Plant Cell **15,** 1242–1256.

Pimpl, P., Movafeghi, A., Coughlan, S., Denecke, J., Hillmer, S., and Robinson, D.G. (2000). *In situ* localization and *in vitro* induction of plant COPI-coated vesicles. Plant Cell **12,** 2219–2236.

Presley, J.F., Cole, N.B., Schroer, T.A., Hirschberg, K., Zaal, K.J., and Lippincott-Schwartz, J. (1997). ER-to-Golgi transport visualized in living cells. Nature **389,** 81–85.

Ritzenthaler, C., Nebenfuhr, A., Movafeghi, A., Stussi-Garaud, C., Behnia, L., Pimpl, P., Staehelin, L.A., and Robinson, D.G. (2002). Reevaluation of the effects of brefeldin A on plant cells using tobacco Bright Yellow 2 cells expressing Golgi-targeted green fluorescent protein and COPI antisera. Plant Cell **14,** 237–261.

Robineau, S., Chabre, M., and Antonny, B. (2000). Binding site of brefeldin A at the interface between the small G protein ADP-ribosylation factor 1 (ARF1) and the nucleotide-exchange factor Sec7 domain. Proc. Natl. Acad. Sci. USA **97,** 9913–9918.

Rossanese, O.W., Soderholm, J., Bevis, B.J., Sears, I.B., O'Connor, J., Williamson, E.K., and Glick, B.S. (1999). Golgi structure corre-lates with transitional endoplasmic reticulum organization in *Pichia pastoris* and *Saccharomyces cerevisiae*. J. Cell Biol. **145,** 69–81.

Rowe, T., Aridor, M., McCaffery, J.M., Plutner, H., Nuoffer, C., and Balch, W.E. (1996). COPII vesicles derived from mammalian endoplasmic reticulum microsomes recruit COPI. J. Cell Biol. **135,** 895–911.

Saint-Jore, C.M., Evins, J., Batoko, H., Brandizzi, F., Moore, I., and Hawes, C. (2002). Redistribution of membrane proteins between the Golgi apparatus and endoplasmic reticulum in plants is reversible and not dependent on cytoskeletal networks. Plant J. **29,** 661–678.

Salama, N.R., Chuang, J.S., and Schekman, R.W. (1997). Sec31 encodes an essential component of the COPII coat required for transport vesicle budding from the endoplasmic reticulum. Mol. Biol. Cell **8,** 205–217.

Salama, N.R., Yeung, T., and Schekman, R.W. (1993). The Sec13p complex and reconstitution of vesicle budding from the ER with purified cytosolic proteins. EMBO J. **12,** 4073–4082.

Sambrook, J., Fritsch, E.F., and Maniatis, T. (1989). Molecular Cloning: A Laboratory Manual. (Cold Spring Harbor, NY: Cold Spring Harbor Laboratory Press).

Scales, S.J., Pepperkok, R., and Kreis, T.E. (1997). Visualization of ER-to-Golgi transport in living cells reveals a sequential mode of action for COPII and COPI. Cell **90,** 1137–1148.

Shima, D.T., Cabrera-Poch, N., Pepperkok, R., and Warren, G. (1998). An ordered inheritance strategy for the Golgi apparatus: Visualization of mitotic disassembly reveals a role for the mitotic spindle. J. Cell Biol. **141,** 955–966.

Springer, S., and Schekman, R. (1998). Nucleation of COPII vesicular coat complex by endoplasmic reticulum to Golgi vesicle SNAREs. Science **281,** 698–700.

Takeuchi, M., Ueda, T., Sato, K., Abe, H., Nagata, T., and Nakano, A. (2000). A dominant negative mutant of sar1 GTPase inhibits protein transport from the endoplasmic reticulum to the Golgi apparatus in tobacco and *Arabidopsis* cultured cells. Plant J. **23,** 517–525.

Takeuchi, M., Ueda, T., Yahara, N., and Nakano, A. (2002). Arf1 GTPase plays roles in the protein traffic between the endoplasmic reticulum and the Golgi apparatus in tobacco and *Arabidopsis* cultured cells. Plant J. **31,** 499–515.

Ward, T.H., Polishchuk, R.S., Caplan, S., Hirschberg, K., and Lippincott-Schwartz, J. (2001). Maintenance of Golgi structure and function depends on the integrity of ER export. J. Cell Biol. **155,** 557–570.

Weissman, J.T., Aridor, M., and Balch, W.E. (2001). Purification and properties of rat liver Sec23-Sec24 complex. Methods Enzymol. **329,** 431–438.

Zaal, K.J., Smith, C.L., Polishchuk, R.S., Altan, N., Cole, N.B., Ellenberg, J., Hirschberg, K., Presley, J.F., Roberts, T.H., Siggia, E., Phair, R.D., and Lippincott-Schwartz, J. (1999). Golgi membranes are absorbed into and reemerge from the ER during mitosis. Cell **99,** 589–601.